



HAL
open science

**The platinum (II) complex
[Pt(O,O'-acac)(γ -acac)(DMS)] alters the intracellular
calcium homeostasis in MCF-7 breast cancer cells**

Antonella Muscella, Nadia Calabriso, Carla Vetrugno, Francesco Paolo Fanizzi, Sandra Angelica De Pascali, Carlo Storelli, Santo Marsigliante

► **To cite this version:**

Antonella Muscella, Nadia Calabriso, Carla Vetrugno, Francesco Paolo Fanizzi, Sandra Angelica De Pascali, et al.. The platinum (II) complex [Pt(O,O'-acac)(γ -acac)(DMS)] alters the intracellular calcium homeostasis in MCF-7 breast cancer cells. *Biochemical Pharmacology*, 2010, 81 (1), pp.91. 10.1016/j.bcp.2010.09.012 . hal-00642427

HAL Id: hal-00642427

<https://hal.science/hal-00642427>

Submitted on 18 Nov 2011

HAL is a multi-disciplinary open access archive for the deposit and dissemination of scientific research documents, whether they are published or not. The documents may come from teaching and research institutions in France or abroad, or from public or private research centers.

L'archive ouverte pluridisciplinaire **HAL**, est destinée au dépôt et à la diffusion de documents scientifiques de niveau recherche, publiés ou non, émanant des établissements d'enseignement et de recherche français ou étrangers, des laboratoires publics ou privés.

Accepted Manuscript

Title: The platinum (II) complex
[Pt(O,O'-acac)(γ -acac)(DMS)] alters the intracellular calcium
homeostasis in MCF-7 breast cancer cells

Authors: Antonella MUSCELLA, Nadia CALABRISO, Carla
VETRUGNO, Francesco Paolo FANIZZI, Sandra Angelica
DE PASCALI, Carlo STORELLI, Santo MARSIGLIANTE



PII: S0006-2952(10)00695-7
DOI: doi:10.1016/j.bcp.2010.09.012
Reference: BCP 10717

To appear in: *BCP*

Received date: 16-7-2010
Revised date: 10-9-2010
Accepted date: 13-9-2010

Please cite this article as: MUSCELLA A, CALABRISO N, VETRUGNO C, FANIZZI FP, PASCALI SADE, STORELLI C, MARSIGLIANTE S, The platinum (II) complex [Pt(O,O'-acac)(γ -acac)(DMS)] alters the intracellular calcium homeostasis in MCF-7 breast cancer cells, *Biochemical Pharmacology* (2010), doi:10.1016/j.bcp.2010.09.012

This is a PDF file of an unedited manuscript that has been accepted for publication. As a service to our customers we are providing this early version of the manuscript. The manuscript will undergo copyediting, typesetting, and review of the resulting proof before it is published in its final form. Please note that during the production process errors may be discovered which could affect the content, and all legal disclaimers that apply to the journal pertain.

The platinum (II) complex [Pt(O,O'-acac)(γ -acac)(DMS)] alters the intracellular calcium homeostasis in MCF-7 breast cancer cells

Antonella **MUSCELLA**¹, Nadia **CALABRISO**², Carla **VETRUGNO**²,
Francesco Paolo **FANIZZI**³, Sandra Angelica **DE PASCALI**³, Carlo **STORELLI**²,
& Santo **MARSIGLIANTE**²

¹Cell Pathology Lab

²Cell Physiology Lab

³General and Inorganic Chemistry Lab

all from the

Dipartimento di Scienze e Tecnologie Biologiche e Ambientali (Di.S.Te.B.A.), Università di
Lecce, Italy

Running Title:

a Pt(II) compound alters the cell Ca²⁺ homeostasis

Correspondence

relating to this paper can be sent to
Professor S Marsigliante at santo.marsigliante@unile.it

Key words: [Pt(O,O'-acac)(γ -acac)(DMS)], [Ca²⁺]_i homeostasis, PMCA, PKC- α , ROS,
MCF-7, ATP

alphabetical list of non-standard abbreviations

CCE, capacitative calcium entry
DMEM, Dulbecco's modification of Eagle's medium;
DMS, dimethylsulphide;
ECL, enhanced chemiluminescence
NBT, nitroblue tetrazolium
PBS, phosphate-buffered saline
PKC- α , protein kinase C-alpha
PMCA, plasma membrane calcium ATPase
PVDF, polyvinylidene difluoride membrane
ROS, reactive oxygen species
SDS, sodium dodecyl sulphate

Abstract

1
2
3
4 It was previously demonstrated that [Pt(O,O'-acac)(γ -acac)(DMS)] exerted toxic effects at
5 high doses, whilst sub-cytotoxic concentrations induced anoikis and decreased cell
6 migration. Aim of this study was to investigate the hypothesis that [Pt(O,O'-acac)(γ -
7 acac)(DMS)] alters the $[Ca^{2+}]_i$ and that this is linked to its ability to trigger rapid apoptosis
8 in MCF-7 cells. Thus, cells were treated with [Pt(O,O'-acac)(γ -acac)(DMS)] and its effects
9 on some of the systems regulating Ca^{2+} homeostasis were studied, also in cells dealing
10 with the complex changes occurring during the Ca^{2+} signalling evoked by extracellular
11 stimuli. [Pt(O,O'-acac)(γ -acac)(DMS)] caused the decrease of PMCA activity (but not
12 SERCA or SPCA) and Ca^{2+} membrane permeability. These two opposite effects on $[Ca^{2+}]_i$
13 resulted in its overall increase from 102 ± 12 nM to 250 ± 24 nM after 15 min incubation.
14 The effects of [Pt(O,O'-acac)(γ -acac)(DMS)] were also evident when cells were stimulated
15 with ATP: the changes in Ca^{2+} levels caused by purinergic stimulation resulted altered due
16 to decreased PMCA activity and to the closure of Ca^{2+} channels opened by purinergic
17 receptor. Conversely, [Pt(O,O'-acac)(γ -acac)(DMS)] did not affect the store-operated Ca^{2+}
18 channels opened by thapsigargin or by ATP. [Pt(O,O'-acac)(γ -acac)(DMS)] provoked the
19 activation of PKC- α and the production of ROS that were responsible for the Ca^{2+}
20 permeability and PMCA activity decrease, respectively. The overall effect of [Pt(O,O'-
21 acac)(γ -acac)(DMS)] is to increase the $[Ca^{2+}]_i$, an effect that is likely to be linked to its
22 ability to trigger rapid apoptosis in MCF-7 cells. These data reinforce the notion that
23 [Pt(O,O'-acac)(γ -acac)(DMS)] would be a promising drug in cancer treatment.
24
25
26
27
28
29
30
31
32
33
34
35
36
37
38
39
40
41
42
43
44
45
46
47
48
49
50
51
52
53
54
55
56
57
58
59
60
61
62
63
64
65

1. Introduction

1
2 Free intracellular Ca^{2+} , acting as a second messenger, is crucial for a diverse range of
3 biological functions, such as fertilization, neurotransmission, muscle contraction, and gene
4 transcription [1]. Intracellular Ca^{2+} signalling is also a key regulator of proliferation [2], cell
5 cycle progression [3], and apoptosis [4].
6
7

8
9 Although the essential role of Ca^{2+} signalling in maintaining homeostatic functions is well
10 established, less is known about the role of aberrant Ca^{2+} signalling in disease [5,6]. In the
11 past decade there has been a realization that particular cancers are associated with
12 alterations in specific Ca^{2+} channels or pumps. Ca^{2+} signalling is involved in various
13 tumorigenic pathways, and the inhibition or activation of specific Ca^{2+} channels or pumps
14 can reduce cellular proliferation and/or induce apoptosis. There is an increasing
15 awareness that PMCA alterations, concurrent with an increase in Ca^{2+} influx channel
16 expression and TRPV6 [7], are associated with tumorigenesis, including that of the
17 mammary gland [8]. Indeed, relative PMCA1 mRNA expression is greater in tumorigenic
18 breast cancer MCF-7 and MDA-MB-231 cells than that in non-tumorigenic MCF-10A cells
19 [9]. PMCA1 and PMCA4 expression is also lower in simian virus 40-transformed human
20 skin fibroblasts [10]. Thus, perturbed PMCA regulation or function may be important in
21 diseases such as cancer. Therapeutic modulation of PMCA expression and/or activity may
22 have functional consequences in suppressing the tumorigenic phenotype. The
23 appropriateness of PMCA as a possible drug target is also demonstrated by the
24 prominence of other clinically used inhibitors of P-type ATPases, digoxin and omeprazole,
25 as inhibitors of Na^+/K^+ -ATPase and H^+/K^+ -ATPase, respectively [11,12]. There are also
26 studies indicating that modulators of Ca^{2+} signalling may offer an effective cell death
27 induction and confer another layer of selectivity for cancer cells with an aberration in
28 multiple Ca^{2+} channels or pumps. For example, tamoxifen alters Ca^{2+} signalling in MCF-7
29 breast cancer cells, and in malignant glioma cell lines it increases cytosolic Ca^{2+} responses
30 to ATP-agonist activation [13]. In glioma cells tamoxifen also increases the radius of Ca^{2+}
31 wave propagation and the rate of Ca^{2+} ionophore-mediated cell death.
32
33

34
35 Recently, this group has synthesized and studied a platinum complex containing two
36 acetylacetonate (acac) ligands, one O,O'-chelate and the other sigma-linked by
37 methionine in gamma position, and dimethyl-sulphide (DMS) in the metal coordination
38 sphere, that has shown interesting biological activities [14]. This compound ($[\text{Pt}(\text{O},\text{O}'\text{-}$
39 $\text{acac})(\gamma\text{-acac})(\text{DMS})]$) not only was able to induce apoptosis in endometrial cancer cells
40 (HeLa), with activity up to about 100 times higher than that of cisplatin, but also showed
41
42
43
44
45
46
47
48
49
50
51
52
53
54
55
56
57
58
59
60
61
62
63
64
65

1 high cytotoxicity in cisplatin resistant MCF-7 breast cancer cells. Differently from cisplatin,
2 for which the activity appears to be associated both with its intracellular accumulation and
3 with the formation of DNA adducts [15,16], the cytotoxicity of this new compound is related
4 to the intracellular accumulation only, showing a low reactivity with nucleobases and a
5 specific reactivity with sulphur ligands, suggesting that the cellular targets could be amino
6 acid residues of proteins.
7

8
9 The different action mechanism of the new complex, having different biological targets,
10 with respect to cisplatin, may render it intrinsically able to evoke less chemo-resistance
11 phenomena. Here we wanted to see whether [Pt(O,O'-acac)(γ -acac)(DMS)] was able to
12 increase the level of free $[Ca^{2+}]_i$ in fura-2-loaded MCF-7 cells. The $[Ca^{2+}]_i$ increase was
13 characterized and the underlying mechanisms were investigated; this study indicates that
14 [Pt(O,O'-acac)(γ -acac)(DMS)] alters the homeostasis of Ca^{2+} thus offering further
15 therapeutic opportunities.
16
17
18
19
20
21
22
23

24 **2. Materials and Methods**

25 **2.1. Determination of $[Ca^{2+}]_i$**

26
27 The medium was aspirated, and the cells were then harvested with 0.05% trypsin-EDTA
28 solution. After washing the cells three times by pelleting (100X g for 5 min), the cells (4 X
29 10⁶) were incubated with 5 μ M fura 2-AM and 0.2% pluronic F-127 for 45 min at 37°C with
30 continuous shaking (100 cycles/min). Following the loading period, the cells were washed
31 twice with a modified Krebs–Ringer buffer in which the bicarbonate was replaced by 20
32 mM Hepes, pH 7.4, incubated again for at least 10 min at room temperature to facilitate
33 hydrolysis of the esterified probe, and washed once again. The cells were resuspended in
34 2 ml of the same buffer containing 0.1% BSA, and 20 μ l of the cell suspension was added
35 to a 2 ml fluorescence cuvette kept at 37°C, and stirred throughout the experiment. The
36 fluorescence intensity was measured with a JASCO FP 750 fluorimeter (Jasco
37 Corporation, Japan). The excitation wavelengths were 340 and 380 nm, and emission was
38 measured at 510 nm. The maximal fluorescence was determined at the end of the assay
39 by adding 20 μ l 10% SDS and the minimal fluorescence by adding 20 μ l 0.5 M EGTA
40 solution, pH 9.0. The cytoplasmic Ca^{2+} concentration at the time t was calculated using the
41 software of the fluorimeter and assuming a dissociation constant for the fura 2- Ca^{2+}
42 complex of 224 nM, according to the Grynkiewicz equation [17]. Mn^{2+} strongly quenched
43 the fura-2 fluorescence at 360 nm. Results are expressed as relative fluorescence
44 quenching with respect to the maximal quenching induced by the addition of digitonin (80
45
46
47
48
49
50
51
52
53
54
55
56
57
58
59
60
61
62
63
64
65

µg/ml).

2.2. Ca²⁺-ATPase activity measurement

ATPase activities were determined by measuring inorganic phosphate (Pi) production by the method of Fiske and Subarrow [18]. This method is based on the reaction between phosphate and molybdate, producing yellow molybdate phosphoric acid which contains a Mo(VI) that is then reduced to Mo(V) present in a blue-coloured heteropolyacid compound. This blue compound is directly measured by reading the absorbance at 700 nm. Ca²⁺-dependent ATPase was measured in crude MCF-7 cell homogenates in the presence of 0.5 mM ouabain and 5 mM sodium azide, potent inhibitor of mitochondrial Ca²⁺ uptake. Typically, 100 µg total cell lysates were incubated for 10 min at 37°C in a reaction mixture consisting of (in mM): 100 NaCl, 20 KCl, 15 Hepes, 12 Tris, 1.2 MgCl₂, 2.5 ATP. This reaction buffer were supplemented with 200 µM CaCl₂ and the free Ca²⁺ concentration (3 µM) has been calculated using the CHELATOR program (BMAXC STANDARD, <http://www.stanford.edu>). The further addition of 1 µM of thapsigargin (to inhibit SERCA activity, [19]), and of 2 µM orthovanadate (a dose used to selectively inhibit PMCA activity freshly prepared to avoid its transformation to decameric vanadate species, [20]) and of 800 µM EGTA (to measure the Mg²⁺-ATPase activity) were made in three different steps, and the activity was measured after each addition in order to evaluate the contribution of each ATPase to the total ATPase activity. The total Ca²⁺-ATPase activity (i.e. the sum of SERCA, PMCA, and SPCA) was obtained after subtraction of the Mg²⁺-ATPase activity from the (Ca²⁺+ Mg²⁺)-ATPase activity obtained immediately after the addition of ATP. The SERCA activity was calculated by subtracting the activity measured in the presence of thapsigargin (which includes PMCA, SPCA, and Mg²⁺-ATPase activities) from the total (Ca²⁺+ Mg²⁺)-ATPase activity. The SPCA activity was calculated by subtracting the Mg²⁺-ATPase activity from the activity in the presence of thapsigargin and vanadate. The PMCA activity was calculated by subtracting the Mg²⁺-ATPase activity and the SPCA activity from the activity in the presence of thapsigargin. Comparable results were obtained when PMCA activity was measured by using carboxyeosin, frequently mentioned as PMCA inhibitor [21].

2.3. Preparation of subcellular fraction.

To obtain protein cell extracts and subcellular fractions we used a procedure previously described [22]. Cells were washed twice in ice-cold PBS and harvested in 1 ml of PBS. The samples were centrifuged for 30 s at 10,000 g, and cell pellets were resuspended in

1
2
3
4
5
6
7
8
9
10
11
12
13
14
15
16
17
18
19
20
21
22
23
24
25
26
27
28
29
30
31
32
33
34
35
36
37
38
39
40
41
42
43
44
45
46
47
48
49
50
51
52
53
54
55
56
57
58
59
60
61
62
63
64
65

the following buffer (mM): 20 Tris–HCl, pH 8, containing 100 NaCl, 2 EDTA, 2 Na₃VO₄, 0.2% Nonidet P-40 and 10% glycerol, supplemented with a cocktail of protease inhibitors. After a 10 min incubation on ice, cells were passed several times through a 20 gauge syringe and then centrifuged at 13,000 g for 10 min at 4 °C. For preparation of subcellular fractions cells were ruptured in homogenization buffer (mM): 20 Tris HCl, pH 7.5, containing 250 sucrose, 2 EDTA, 0.5 EGTA, 0.2 phenylmethylsulfonyl fluoride and a cocktail of protease inhibitors, by Dounce homogenization and centrifuged immediately at 2,000 g for 10 min. The supernatant was collected and centrifuged at 100,000 g for 1 hr to separate cytosolic and membrane fractions. The membrane fraction was subsequently resuspended in extraction buffer (mM): 20 Tris HCl, pH 7.5, containing 150 NaCl, 1 EDTA, 1 EGTA, and a cocktail of protease inhibitors (containing 0.2 mM phenylmethylsulfonyl fluoride, 10 µg/ml aprotinin, 10 µg/ml soybean trypsin inhibitor and 10 µg/ml leupeptin) with 1% (vol/vol) Nonidet P-40. Nuclei were pelleted by centrifugation at 2,000 g for 15 min at 4°C and resuspended in high-salt buffer (mM): 20 Tris–HCl, pH 7.9, 420 NaCl, 10 KCl, 0.1 Na₃VO₄, 1 EDTA, 1 EGTA, 20% glycerol, supplemented with a cocktail of protease inhibitors, and sonicated until no nuclei remained intact. Samples were then centrifuged at 13,000 g for 10 min at 4 °C, and the resultant supernatant was used as the nuclear extract. The purity of fractions was tested by immunoblotting with antibodies specific to α -Na⁺/K⁺ ATPase subunity (membrane protein) and β -actin (cytoplasmic protein). Proteins in the homogenates and cellular fraction were determined using the Bio-Rad protein assay kit 1. Lyophilized bovine serum albumin was used as a standard.

2.4. Western blot analysis.

Proteins in homogenates and cellular fraction were determined using the Bio-Rad protein assay kit 1 (Milan, Italy). Lyophilised bovine serum albumin was used as a standard. Total cell proteins or proteins of the distinct sub-cellular fractions were dissolved in SDS sample buffer and separated on 10% or 15% SDS gels. Separated proteins were transferred electrophoretically onto polyvinylidene difluoride membrane (PVDF) (Amersham International). Equal protein loading was confirmed by Ponceau S staining. Blots were incubated with specific primary antibodies and the immune complexes were detected using appropriate peroxidase conjugated secondary antibodies and enhanced chemiluminescent detection reagent ECL (Amersham International). Blots were stripped and used for sequential incubations with relative control antibody (α -Na⁺/K⁺ATPase subunity for membrane protein and β -actin for cytoplasmic protein). Densitometric analysis was carried out on Western blots using the NIH Image (v1.63) software. The pixel intensity

for each region was analyzed, the background was subtracted, and the protein expressions were normalized to β -actin loading control for each lane.

2.5. Intracellular reactive oxygen species (ROS) formation.

ROS generation was detected by nitroblue tetrazolium (NBT) assay as previously described [22]. NBT (1 mg/ml) was added to medium of treated MCF-7 and incubations were carried out at 37 °C for 15–60 min. NBT is reduced by ROS to a dark blue insoluble form of NBT called formazan. Cells were then carefully washed and lysed in a 90% dimethylsulfoxide solution containing 0.01 N NaOH and 0.1% SDS. Absorbance of formazan was measured at 550 nm against lysis buffer blank. Data are expressed as % of control untreated MCF-7 cells.

2.6. Anion superoxide ($O_2^{\cdot-}$) production.

$O_2^{\cdot-}$, the main free radical produced in mitochondria, was measured using the cell-permeable probe MitoSOX Red. The reduced probe is taken up by cells and in the presence of $O_2^{\cdot-}$ is oxidized and becomes fluorescent, emitting a red fluorescence after 488 nm laser excitation. After treatment with the drug, cells were incubated for 10 minutes with MitoSOX Red reagent 5 μ M in 0.5 ml of Hank's Balanced Salt Solution with calcium and magnesium ($CaCl_2$ 140 mg/L, $MgCl_2 \cdot 6H_2O$ 10 mg/L and $MgSO_4 \cdot 7H_2O$ 10 mg/L) at 37 °C. After washing twice, adhered cells were observed (maximum excitation/emission of MitoSOX reagent: 510/580nm) and images and values of fluorescence were obtained by fluorescence microscopy as mean fluorescence intensities (MFI/cell).

2.7. Statistical analysis.

Experimental points represent means \pm standard deviation (S.D.) of 3–6 replicates. Statistical analysis was carried out using the ANOVA. When indicated, post hoc tests (Bonferroni/Dunn) were also performed. A p value less than 0.05 was considered to achieve statistical significance.

2.8. Reagents and MCF-7 cell line.

The PKC inhibitors GF109203X and Gö6976 were obtained from Calbiochem (Darmstadt, Germany). Fura 2-AM and thapsigargin were from Molecular Probes (Eugene, OR, USA). Antibodies used in western analyses to PKC- α , - ϵ , - δ , - ι and - ζ , β -actin and α -subunit of Na^+/K^+ ATPase, goat anti-rabbit IgG conjugated with peroxidase, as well as control

antibodies, were obtained from Santa Cruz Biotechnology (Santa Cruz, CA, USA). The inhibitors of NADPH oxidase, diphenyleneiodonium (DPI) and apocynin, nitroblue tetrazolium (NBT), MitoSOX Red and all the inorganic salts were obtained from Sigma (Milan, Italy).

MCF-7 cell line was cultured in DMEM (Celbio, Pero, Milan, Italy) supplemented with 10% fetal bovine serum, penicillin (100 U/ml) and streptomycin (100 mg/ml). Cells were grown to 70% confluence and then treated with [Pt(O,O'-acac)(γ -acac)(DMS)] at various concentrations and for different incubation periods.

3. RESULTS

3.1. Effects of [Pt(O,O'-acac)(γ -acac)(DMS)] on $[Ca^{2+}]_i$

We showed previously that the new Pt complex containing an O,O'-chelated acetylacetonate ligand (acac) and a dimethyl-sulphide in the Pt coordination sphere, [Pt(O,O'-acac)(γ -acac)(DMS)], induces apoptosis in MCF-7 breast cancer cell line, relatively insensitive to cisplatin. In contrast to cisplatin, the cytotoxicity of [Pt(O,O'-acac)(γ -acac)(DMS)] correlated with cellular accumulation but not with DNA binding, as it activates the mitochondrial apoptotic pathway [16]. In many cases, an early and pivotal event in apoptosis is a cytosolic free Ca^{2+} concentration ($[Ca^{2+}]_i$) increase. To determine whether this was an early event during [Pt(O,O'-acac)(γ -acac)(DMS)], induced apoptosis, we first examined whether intracellular $[Ca^{2+}]_i$ levels increased in MCF-7 cells after [Pt(O,O'-acac)(γ -acac)(DMS)] exposure, using fura-2-AM in a spectrofluorometric assay. In MCF-7 cells, the basal level of $[Ca^{2+}]_i$ was 102 ± 7 nM (mean \pm S.D.; n=30). MCF-7 cells were incubated for different times (1 - 20 min) with crescent concentrations of [Pt(O,O'-acac)(γ -acac)(DMS)]. The treatment with [Pt(O,O'-acac)(γ -acac)(DMS)] increases $[Ca^{2+}]_i$ in dose-dependent manner (Fig. 1A); between 0.5 and 10 μ M, the increase in $[Ca^{2+}]_i$ ranged from 145 ± 10 nM to 250 ± 24 nM. Concentrations above 10 μ M were not tested because they are clinically irrelevant. In MCF-7 cells, the increase in $[Ca^{2+}]_i$ was restricted to [Pt(O,O'-acac)(γ -acac)(DMS)] since cisplatin and carboplatin (up to a concentration of 100 μ M), did not elevate $[Ca^{2+}]_i$ (Fig. 1B and C). While transient elevations of $[Ca^{2+}]_i$ are important signals within cells, prolonged elevations of $[Ca^{2+}]_i$ could be lethal. A $[Ca^{2+}]_i$ overload may activate cell death via apoptosis [4]. Theoretically, there are at least two possibilities for altering $[Ca^{2+}]_i$ homeostasis in MCF-7 cells by [Pt(O,O'-acac)(γ -acac)(DMS)]. Elevation of the $[Ca^{2+}]_i$ can result: a) from Ca^{2+} -influx from the extracellular

space and/or from Ca^{2+} -release from intracellular stores; b) from Calcium-ATPases (PMCA/SERCA/SPCA) and/or the Na^+ - Ca^{2+} -Exchanger (NCX) activity inhibition.

3.2. Effect of [Pt(O,O'-acac)(γ -acac)(DMS)] on Mn^{2+} uptake in MCF-7 cells

To test whether the changes of the $[\text{Ca}^{2+}]_i$ response caused by [Pt(O,O'-acac)(γ -acac)(DMS)] were due to modulation of the plasma membrane permeability, we measured Mn^{2+} influx after the addition of [Pt(O,O'-acac)(γ -acac)(DMS)]. Mn^{2+} is a good Ca^{2+} -entry tracer, since it is not pumped out of the cell [23]. Mn^{2+} uptake was estimated by the quenching of fura-2 fluorescence when excited at 360 nm, which is an isosbestic wavelength and is insensitive to variations in $[\text{Ca}^{2+}]_i$ concentration. Fig. 2A shows the fluorescence quenching by Mn^{2+} influx: the membrane permeability was significantly decrease by [Pt(O,O'-acac)(γ -acac)(DMS)] in a dose-dependent manner (Fig 2B). Mn^{2+} entry was drastically decreased by the impermeant cation La^{3+} (100 μM), an effect similar to that obtained with 10 μM [Pt(O,O'-acac)(γ -acac)(DMS)] (Fig. 2). The effect of 10 μM [Pt(O,O'-acac)(γ -acac)(DMS)] or 100 μM La^{3+} on Mn^{2+} entry was not augmented were both were used in combination (Fig. 2B).

3.3. Inhibitory effects of [Pt(O,O'-acac)(γ -acac)(DMS)] on of Ca^{2+} -ATPases activity

First, Ca^{2+} -dependent ATPase was measured in crude MCF-7 cell homogenates in the presence of 0.5 mM ouabain. The method used to measure Ca^{2+} -dependent ATPase in MCF-7 cells was sensitive and reproducible. In standard culture conditions, the coefficient of variation of a single assay was 3.2% (n=8) and Ca^{2+} -dependent ATPase activities (PMCA, SERCA and SPCA) increased linearly with increasing protein concentrations. Figure 3A presents data on ouabain-insensitive ATP hydrolysis in the presence and absence (obtained adding 800 μM EGTA) of Ca^{2+} . MCF-7 cells clearly catalysed Ca^{2+} -sensitive ATP hydrolysis. Approximately 35% of ouabain-insensitive ATPase activity ($\sim 7.1 \pm 0.3 \mu\text{mol Pi/h/mg/protein}$ as previously shown, [24]) was Ca^{2+} dependent. This activity consisted of the following activities: PMCA ($1.12 \pm 0.11 \mu\text{mol Pi/h/mg/protein}$), SERCA ($0.63 \pm 0.11 \mu\text{mol Pi/h/mg/protein}$ and SPCA ($0.16 \pm 0.13 \mu\text{mol Pi/h/mg/protein}$) (all the activities were mean \pm S.D. of five independent experiments, Fig.3A). [Pt(O,O'-acac)(γ -acac)(DMS)] (0.1-10 μM) had no effects on SERCA activity (Fig. 3B), nor on that of the SPCA (data not shown). Conversely, [Pt(O,O'-acac)(γ -acac)(DMS)] produced a significant decrease in PMCA activity in a dose- and time-dependent manner (ANOVA: $P < 0.0001$; Fig. 3B and C). The maximal effect, in sub-confluent conditions, was obtained after 10

minutes of incubation with 10 μM [Pt(O,O'-acac)(γ -acac)(DMS)], and corresponded to a 1.6-fold decrement in PMCA activity.

3.4. Effects of [Pt(O,O'-acac)(γ -acac)(DMS)] on ATP-induced Ca^{2+} response in MCF-7 cells

In order to understand whether the effects provoked by [Pt(O,O'-acac)(γ -acac)(DMS)] had an effective role in controlling the homeostasis of intracellular calcium, we provoked physiological disturbances in $[\text{Ca}^{2+}]_i$ using ATP, an agonist able to induce intracellular calcium signalling in MCF-7 cells, due to stimulation of phospholipase C through P2Y2 receptors [25]. The $[\text{Ca}^{2+}]_i$ transient evoked by ATP consisted of a rapid peak followed by a sustained phase of elevated $[\text{Ca}^{2+}]_i$, which persisted for over 3 min (Fig. 4A). The maximum increase in $[\text{Ca}^{2+}]_i$ was observed at 100 μM ATP, with a $[\text{Ca}^{2+}]_i$ of 509 ± 21 nM. ATP-induced $[\text{Ca}^{2+}]_i$ transients were then examined in the presence of increasing [Pt(O,O'-acac)(γ -acac)(DMS)] concentrations (0.5 - 10 μM). As shown in Fig. 4A, in a first phase lasting about 1 min, 10 μM [Pt(O,O'-acac)(γ -acac)(DMS)] significantly decreased the peak of $[\text{Ca}^{2+}]_i$ (from 509 ± 21 nM to 440 ± 18 nM, $n = 7$; $p < 0.001$); afterwards, it increased, in a dose-dependent manner, both the rate of the Ca^{2+} decline and the post-stimulatory $[\text{Ca}^{2+}]_i$ level, calculated after 3 min from ATP administration. In order to quantify the effect of [Pt(O,O'-acac)(γ -acac)(DMS)] on such ATP-evoked Ca^{2+} transient, the variations in Ca^{2+} profile were also evaluated both as b/a ratio and as Ca^{2+} rate of decline. Precisely, we expressed the $[\text{Ca}^{2+}]_i$ observed after 2 min from stimulation (b), as a fraction of $[\text{Ca}^{2+}]_i$ peak (a) (Fig. 4B *in set*), and the b/a ratio was calculated for the different concentrations (0.5–10 μM). Figure 4B shows that under control conditions (i.e., exposure to ATP alone) (b) was 30% of peak $[\text{Ca}^{2+}]_i$. When applied together with ATP, [Pt(O,O'-acac)(γ -acac)(DMS)] increased, in a dose dependent manner, the b/a ratio (Fig. 4B). The effect provoked by the channel blocker La^{3+} (100 μM), was very different from the effect of 10 μM [Pt(O,O'-acac)(γ -acac)(DMS)] (Fig. 4B and C), inasmuch as, while they both were able to strongly reduce the Ca^{2+} entry, La^{3+} , differently from [Pt(O,O'-acac)(γ -acac)(DMS)], had no effect on PMCA activity. This suggests that the increase in the b/a ratio caused by [Pt(O,O'-acac)(γ -acac)(DMS)] is mainly due to inhibition of the pump rather than the decrease of plasma membrane permeability. Obviously, [Pt(O,O'-acac)(γ -acac)(DMS)]-treated cells had a slower rate of PMCA-mediated free intracellular Ca^{2+} efflux. The rate of decline, assayed in a time interval of 1 min after the peak, could be a relative measure of PMCA-mediated free intracellular Ca^{2+} efflux. The rates of decline in $[\text{Ca}^{2+}]_i$ obtained with

1 the various [Pt(O,O'-acac)(γ -acac)(DMS)] concentrations were plotted against the relative
2 [Ca²⁺]_i peak values, for comparisons of PMCA-mediated Ca²⁺ efflux rates (Fig. 4D). In
3 order to discriminate between the effects on plasma membrane channels and PMCA
4 inhibition provoked by [Pt(O,O'-acac)(γ -acac)(DMS)] and those due to the channel closure
5 only, the rate of decline in [Ca²⁺]_i obtained with 100 μ M La³⁺ was also evaluated; as shown
6 in Fig. 4D, La³⁺ provoked a rate of Ca²⁺ decline and a Ca²⁺ peak value significantly
7 different from those provoked by [Pt(O,O'-acac)(γ -acac)(DMS)]. Since PMCA activity is
8 known to be Ca²⁺-dependent, MCF-7 cells were treated or not, for the indicated times, with
9 100 μ M ATP and then Ca²⁺-ATPase activity was assayed. ATP stimulated PMCA activity by
10 about 50% after 2.5 min incubation and [Pt(O,O'-acac)(γ -acac)(DMS)] significantly
11 decreased the activity of the ATP-stimulated PMCA (Fig. 3D). The origin of the ATP-
12 induced Ca²⁺ sustained phase was studied using a Ca²⁺-free medium obtained substituting
13 2 mM MgCl₂ for 2 mM CaCl₂ in the standard experimental medium previously passed
14 through a Chelex 100 column. In these experimental conditions, the effect of ATP on peak
15 height was much less pronounced with respect to that obtained in the presence of Ca²⁺-
16 containing solution ([Ca²⁺]_i peak decreased from 509 \pm 21 nM to 286 \pm 12 nM (p < 0.001).
17 Figure 5A shows an example of a [Ca²⁺]_i transient evoked by bath application of ATP (100
18 μ M) in Ca²⁺-free external solution. The ATP-induced [Ca²⁺]_i transient was characterized by
19 a rapid and pronounced initial rise that then declined completely to the pre-stimulatory
20 level. When ATP was applied simultaneously with [Pt(O,O'-acac)(γ -acac)(DMS)], the
21 [Ca²⁺]_i transient appeared significantly wide and decelerated (Fig. 5B). In MCF-7 cells, the
22 pathway that links purinoceptors to intracellular Ca²⁺ release involves the InsP3 signalling
23 cascade [26]; such Ca²⁺ release then results in external Ca²⁺ entry. Thus, we investigated
24 whether the InsP3-dependent Ca²⁺ release was involved in the [Pt(O,O'-acac)(γ -
25 acac)(DMS)]-induced [Ca²⁺]_i increase by using 2-aminoethoxydiphenyl borate (2-APB), a
26 membrane-permeant InsP3R blocker [27]. Cells incubated with 20 μ M 2-APB 10 min
27 before the stimulation with 100 μ M ATP, in Ca²⁺-free conditions, led to a significant
28 reduction (by 62 \pm 6%, n=5, P < 0.05) of the amplitude of the ATP-induced [Ca²⁺]_i transient
29 (Fig. 5A and C), confirming prior observations showing that the ATP induced [Ca²⁺]_i
30 transient is due to Ca²⁺ release through InsP3Rs [28]. Afterwards, cells were incubated
31 with 20 μ M 2-APB for 10 min and then stimulated with ATP together with [Pt(O,O'-acac)(γ -
32 acac)(DMS)]: again, a significant inhibition of the [Ca²⁺]_i transient (by 68 \pm 5%, n=5, P
33 < 0.05) was obtained (Fig. 5B and C), similar to that obtained in the absence of [Pt(O,O'-
34 acac)(γ -acac)(DMS)], therefore suggesting that [Pt(O,O'-acac)(γ -acac)(DMS)] caused an
35 InsP3-independent Ca²⁺ increase. Extracellular Ca²⁺ entry was generated by adding 2 mM
36
37
38
39
40
41
42
43
44
45
46
47
48
49
50
51
52
53
54
55
56
57
58
59
60
61
62
63
64
65

1
2
3
4
5
6
7
8
9
10
11
12
13
14
15
16
17
18
19
20
21
22
23
24
25
26
27
28
29
30
31
32
33
34
35
36
37
38
39
40
41
42
43
44
45
46
47
48
49
50
51
52
53
54
55
56
57
58
59
60
61
62
63
64
65

CaCl₂ to the Ca²⁺-free buffer after recovery of the ATP-induced [Ca²⁺]_i transient. The combined administration of ATP and [Pt(O,O'-acac)(γ-acac)(DMS)] (10 μM) reduced from 284 ± 10 nM to 265 ± 9 nM (p<0.001; n = 6) the peak height of extracellular Ca²⁺ entry (Fig. 5B). 2-APB (20 μM) completely abolished the extracellular Ca²⁺ entry in cells stimulated with ATP alone or with ATP plus [Pt(O,O'-acac)(γ-acac)(DMS)] (Fig. 5).

3.5. Effect of [Pt(O,O'-acac)(γ-acac)(DMS)] on thapsigargin-evoked extracellular Ca²⁺ entry.

Thapsigargin, an inhibitor of the SERCA, allows Ca²⁺ to leak out from the ER pool [19] causing complete store depletion also in MCF-7 cells [29]. The simultaneous administration of thapsigargin and [Pt(O,O'-acac)(γ-acac)(DMS)] to MCF-7 cells, kept in Ca²⁺-free medium, increased the [Ca²⁺]_i peak, probably as a consequence of the decreased PMCA activity (Fig. 6B and C). In fact, a similar [Ca²⁺]_i increase was also obtained by pretreatment of cells with orthovanadate ([VO₃(OH)]₂), a PMCA inhibitor [20] (Fig. 6B and C). Furthermore, differences in extracellular Ca²⁺ entry obtained by thapsigargin, in the presence and in the absence of [Pt(O,O'-acac)(γ-acac)(DMS)], were also observed (Fig. 6B and D). However, the effects of [Pt(O,O'-acac)(γ-acac)(DMS)] on extracellular Ca²⁺ entry due to ATP or thapsigargin were different (Fig. 6A and D). The effects of [Pt(O,O'-acac)(γ-acac)(DMS)] on the extracellular Ca²⁺ entry were also evaluated by using the Mn²⁺ quenching technique, since this cation is not transported by the major calcium pumps, SERCA and PMCA. Indeed, the entry of Mn²⁺ increased in both thapsigargin- and ATP-treated cells, resulting however significantly higher when using ATP (Fig. 6 E and F), probably because of the opening of second messengers-operated Ca²⁺ channels, in addition to store-operated channels. When 10 μM [Pt(O,O'-acac)(γ-acac)(DMS)] was administered together with thapsigargin or ATP, the quenching of Mn²⁺ significantly decreased, reaching the same value (Fig. 6F). Taken together, these results suggest that the Ca²⁺/Mn²⁺-permeable plasma membrane channels opened by ATP only are targets of [Pt(O,O'-acac)(γ-acac)(DMS)]. Conversely, the Ca²⁺/Mn²⁺-permeable plasma membrane store-operated channels opened by both ATP and thapsigargin, may not be affected by [Pt(O,O'-acac)(γ-acac)(DMS)].

3.6. Effects of [Pt(O,O'-acac)(γ-acac)(DMS)] on Na⁺/Ca²⁺-Exchanger activity

In order to understand the involvement of a Na⁺/Ca²⁺ exchanger in the [Pt(O,O'-acac)(γ-acac)(DMS)]-induced [Ca²⁺]_i changes, we studied the effects of [Pt(O,O'-acac)(γ-

1 acac)(DMS)] on Ca^{2+} influx using buffers with Na^+ concentrations being 0 and 140 mM.
2 First, the effects of ATP were dependent on Na^+ concentration, since the replacement of
3 extracellular Na^+ with choline, significantly increased the early peak rise in $[\text{Ca}^{2+}]_i$ from 509
4 ± 21 nM to 585 ± 30 nM (ANOVA; $p < 0.001$; $n = 6$, Fig. 7A). Secondly, cells co-stimulated
5 with ATP and [Pt(O,O'-acac)(γ -acac)(DMS)], displayed a lower $[\text{Ca}^{2+}]_i$ peak in the presence
6 of 140 mM Na^+ (450 ± 15 nM, $n = 6$) than in the absence (525 ± 21 nM, $n = 6$, Fig. 7B).
7 Since the difference between the early peak rise in $[\text{Ca}^{2+}]_i$ obtained in physiological and
8 Na^+ -free buffers in the absence or presence of [Pt(O,O'-acac)(γ -acac)(DMS)] is practically
9 identical (Fig. 7C), we may conclude that [Pt(O,O'-acac)(γ -acac)(DMS)] has no effects on
10 the activity of the $\text{Na}^+/\text{Ca}^{2+}$ exchanger.
11
12
13
14
15
16
17
18

19 **3.7. Effects of [Pt(O,O'-acac)(γ -acac)(DMS)]-activated PKC- α on extracellular Ca^{2+}** 20 **entry**

21
22 Protein kinase C (PKC) is known to regulate Ca^{2+} homeostasis through negative feedback
23 mechanisms [30]. Inasmuch as activated PKCs translocate from the cytosol to the cellular
24 membranes, we analysed, by Western blots, the distribution of PKCs expressed by MCF-7
25 (PKC- α , - δ , - ϵ , - ι and - ζ [31]) in cells treated with 10 μM Pt(O,O'-acac)(γ -acac)(DMS)] for
26 different incubation times (0.5, 1, 5, and 10 min). As shown in Fig. 8A, a cytosol-to-
27 membrane translocations of PKC- α , PKC- δ and PKC- ϵ were observed. The involvement of
28 translocating PKCs in the effect of [Pt(O,O'-acac)(γ -acac)(DMS)] on extracellular Ca^{2+}
29 entry was investigated by using the PKC inhibitors GF109203X (able to inhibit all isoforms)
30 and Gö6976 (and inhibitor of conventional, calcium-dependent PKC- α ; note that PKC- α is
31 the only conventional PKC expressed by MCF-7 cells) [32]. Pre-incubation of cells with
32 GF109203X (0.1 and 1 μM for 15 min) (data not shown), or with Gö6976 (1 μM) for 15
33 min, reversed the effects of 10 μM [Pt(O,O'-acac)(γ -acac)(DMS)] on extracellular Ca^{2+}
34 entry (Fig. 8B), suggesting that such effects may be mediated by PKC- α . The role of PKC-
35 α in modulating plasma membrane permeability can also be seen in experiments of Mn^{2+}
36 quenching, where the use of Gö6976 in cells treated with both [Pt(O,O'-acac)(γ -
37 acac)(DMS)] and ATP significantly increased the Mn^{2+} influx (from 5.77 ± 0.22 to $14.70 \pm$
38 $0.46 \Delta_{360}/\text{min}$, $p < 0.05$; $n = 6$), back to values obtained in cells treated with ATP only (Fig.
39 8C). Moreover, Gö6976 reversed the effects of [Pt(O,O'-acac)(γ -acac)(DMS)] on plasma
40 membrane permeability in untreated cells (from 2.19 ± 0.13 to $6.52 \pm 0.26 \Delta_{360}/\text{min}$,
41 $p < 0.05$; $n = 6$, Fig. 8B). These results suggest that [Pt(O,O'-acac)(γ -acac)(DMS)]-activated
42 PKC- α changed the plasmalemma Ca^{2+} permeability interfering with some Ca^{2+} plasma
43 membrane channels.
44
45
46
47
48
49
50
51
52
53
54
55
56
57
58
59
60
61
62
63
64
65

3.8. ROS are responsible for the [Pt(O,O'-acac)(γ -acac)(DMS)]-induced decrease of the PMCA activity.

[Pt(O,O'-acac)(γ -acac)(DMS)] increased the level of ROS in a time-dependent manner with ROS generation significantly different respect to control (ANOVA: $p < 0.005$) as soon as 1 min (Fig. 9A). [Pt(O,O'-acac)(γ -acac)(DMS)]-provoked ROS production was partially inhibited by diphenyleneiodonium (DPI), an inhibitor of the NADPH oxidase (Fig. 9D). Since another important sources of intracellular ROS are mitochondria, we studied the specific production of mitochondrial $O^{\cdot -2}$ by MitoSOX red. We found that [Pt(O,O'-acac)(γ -acac)(DMS)] increased the mitochondrial synthesis of $O^{\cdot -2}$ (Fig. 9B), in a time-dependent manner (Fig. 9C), and that such effect was blocked by the antioxidant apocynin (10 μ M). Apocynin also reversed the [Pt(O,O'-acac)(γ -acac)(DMS)]-provoked inhibition of PMCA activity (Fig. 9E).

3.9 Effects of [Pt(O,O'-acac)(γ -acac)(DMS)] on other human breast cell lines

To determine whether the observations made on MCF-7 cells are also valid for other cell lines, we tested two other breast cancer cell lines, MDA-MB-231 and SKBR-3. Furthermore, we also included the MCF-10A, a nontumorigenic breast epithelial cell that appeared to be less sensitive to [Pt(O,O'-acac)(γ -acac)(DMS)] than MCF-7 cells in cytotoxicity assays [16]. Thus, a selected set of crucial experiments (effects of 10 μ M [Pt(O,O'-acac)(γ -acac)(DMS)] on (a) intracellular $[Ca^{2+}]_i$ levels, (b) membrane permeability, (c) PMCA activity and (d) ROS generation) were performed and the results shown in Table I. The results show that the effect of [Pt(O,O'-acac)(γ -acac)(DMS)] are not significantly different in the three tumor cell lines while, on the contrary, such effects are much less evident, although significant compared with controls, in normal MCF-10A cells.

4. DISCUSSION

Antineoplastic drugs resistance poses a major impediment to the successful treatment of breast cancer. About 70% of breast cancers are oestrogen receptor positive (ER+ve). The remaining 30% are ER-ve [33]. Oestrogen hormone promotes breast cancer cell proliferation through ER, therefore, oestrogen antagonists such as tamoxifen are used to block ER activation in ER+ve breast cancer patients [34]. We have previously synthesized a new Pt complex, [Pt(O,O'-acac)(γ -acac)(DMS)], in the attempt to find novel strategies for a better management of ER-ve breast cancer. This compound may be a promising new

therapeutic agent because it induces apoptosis in MCF-7 breast cancer cell line, relatively insensitive to cisplatin [16]. We have demonstrated that [Pt(O,O'-acac)(γ -acac)(DMS)] decreases Bcl-2 expression in MCF-7 cells and contributes to the formation of pores by facilitating the translocation of Bax, a proapoptotic factor, from the cytosol to the outer mitochondrial membrane [16]. This mechanism, allows the dissipation of mitochondrial membrane potential and the release of cytochrome c and is Ca^{2+} independent [35]. Furthermore, the dissipation of membrane potential minimizes the contribution of mitochondria to Ca^{2+} homeostasis and causes ATP depletion which further increases the $[\text{Ca}^{2+}]_i$ by decreasing the Ca^{2+} pump activities. It is well known that in apoptosis, the appropriateness of Ca^{2+} handling is of fundamental importance [4] with Ca^{2+} playing different roles in this process; for example, Ca^{2+} from the extracellular space, or released from endoplasmic reticulum, leads to an increase in the mitochondrial Ca^{2+} concentration, which results in the increase of transition pore permeability which activates apoptosis [6]. It is well established that altered expression of specific Ca^{2+} channels and pumps are characteristic features of some cancers and anticancer drugs such as cisplatin, are able to increase $[\text{Ca}^{2+}]_i$ through various mechanisms [36-38]. We here show that [Pt(O,O'-acac)(γ -acac)(DMS)] evokes an early increase in $[\text{Ca}^{2+}]_i$ (Fig. 1A). This supports the hypothesis that homeostatic mechanisms involved in the regulation of $[\text{Ca}^{2+}]_i$ may play a role during [Pt(O,O'-acac)(γ -acac)(DMS)]-induced apoptosis. The increase of $[\text{Ca}^{2+}]_i$ provoked by [Pt(O,O'-acac)(γ -acac)(DMS)] does not depend on the external Ca^{2+} concentration (Figs. 5 and 6). Indeed, [Pt(O,O'-acac)(γ -acac)(DMS)] decreased the permeability of the plasma membrane, an effect that is comparable to that caused by La^{3+} (Fig. 2). This increase could be caused by the action of [Pt(O,O'-acac)(γ -acac)(DMS)] on at least one of the various systems that regulate Ca^{2+} homeostasis, such as Ca^{2+} transport pumps (the plasma membrane Ca^{2+} -ATPases PMCA, the sarco/endoplasmic reticulum Ca^{2+} -ATPases SERCA, and the secretory pathway Ca^{2+} -ATPases SPCA), and secondary $\text{Na}^+/\text{Ca}^{2+}$ antiporter. We have shown that both SPCA and SERCA activities were not affected by the treatment with [Pt(O,O'-acac)(γ -acac)(DMS)] (Fig. 3). The PMCA removes the Ca^{2+} through the plasma membrane and is important for the maintenance of basal levels of cytosolic Ca^{2+} and lowering of $[\text{Ca}^{2+}]_i$ after the generation of Ca^{2+} transients [1]. Measuring the ATPase activity gave a direct indication that PMCA was inhibited by Pt(O,O'-acac)(γ -acac)(DMS)] (Fig. 3). This inhibition resulted in changes in the ATP-induced $[\text{Ca}^{2+}]_i$ profile. These changes are clearly due mainly to the combined effects of [Pt(O,O'-acac)(γ -acac)(DMS)] on permeability and PMCA activity. Since the effects of inhibition of PMCA occurred slowly (Fig. 3C), compared to changes in permeability (Figs. 2, 6E and 8C),

1 these latter changes became more important in the second phase of the transient, causing
2 an overall rise in Ca^{2+} level. Clearly, PMCA represents a potential therapeutic target, since
3 its inhibition affects the efflux of Ca^{2+} by increasing its concentration that may eventually
4 lead to the induction of apoptosis. In this regard it has been shown that even the partial
5 inhibition of PMCA-mediated Ca^{2+} efflux is sufficient to reduce proliferation of MCF-7 cells
6 [38]. Furthermore, an antisense construct directed towards PMCA leads to changes in cell-
7 cycle kinetics, such as lengthening the G2 phase and simultaneously reducing the Ca^{2+}
8 efflux [39]. PMCA is a very sensitive target for oxidative stress as occurs in pancreatic
9 acinar cells [40] and in neuronal and liver membranes [41,42]. We have noticed that
10 addition of [Pt(O,O'-acac)(γ -acac)(DMS)] to MCF-7 cells induces rapid production of ROS
11 (Fig. 9A and C). It is known that ROS can be produced through the activation of NAD(P)H
12 oxidase, or mitochondrial pathways [43]. Therefore, it is expected that the origin of the
13 ROS in cells treated with [Pt(O,O'-acac)(γ -acac)(DMS)] is twofold: primarily by NAD(P)H
14 oxidase, but also by mitochondria (with apocynin inhibiting this effect, Fig. 9B). In fact,
15 whilst the inhibition of NAD(P)H oxidase by DPI only partially prevented [Pt(O,O'-acac)(γ -
16 acac)(DMS)]-induced ROS generation, the use of the antioxidant apocynin inhibited this
17 effect (Fig. 9D) and restored the PMCA activity due to ROS production (Fig. 9E). The
18 effects of ROS on PMCA could be due to either the aggregation of PMCA molecules, as a
19 result of Cys oxidation to disulphides and increased hydrophobic interactions [41], or to the
20 increase of $[\text{Ca}^{2+}]_i$ due to the oxidative stress which activates Ca^{2+} -dependent proteases,
21 such as caspases, known to make PMCA inactive [44, 45]. A somewhat similar mechanism
22 has been described in neurons, whereby cleavage of the $\text{Na}^+/\text{Ca}^{2+}$ exchanger by caspases
23 was shown to mediate the Ca^{2+} overload during the excitotoxicity associated with brain
24 ischemia [46]. However, we show that the effects of [Pt(O,O'-acac)(γ -acac)(DMS)] on
25 $[\text{Ca}^{2+}]_i$ are not due to modulation of the $\text{Na}^+/\text{Ca}^{2+}$ exchanger activity (Fig. 7). It seems that
26 the mechanism dependent on caspase activation does not occur in our case. This
27 conclusion is based upon previous results [16] which show that the time frame over which
28 caspases became significantly activated by [Pt(O,O'-acac)(γ -acac)(DMS)] occurred much
29 later compared to the inactivation of PMCA, which is already evident after 30-sec exposure
30 to [Pt(O,O'-acac)(γ -acac)(DMS)] (Fig. 3C). Consequently, the anti-neoplastic potential of
31 [Pt(O,O'-acac)(γ -acac)(DMS)] might also be based on its ability to produce changes in
32 Ca^{2+} homeostasis, like others pump inhibitors. We have tried to estimate the possible
33 effect of [Pt(O,O'-acac)(γ -acac)(DMS)] on the membrane permeability to Ca^{2+} . A raise in
34 the $[\text{Ca}^{2+}]_i$ can be due to Ca^{2+} -influx from the extracellular space or Ca^{2+} -release from
35 intracellular stores [5,47]. Channels mediating Ca^{2+} -influx from the extracellular space are
36
37
38
39
40
41
42
43
44
45
46
47
48
49
50
51
52
53
54
55
56
57
58
59
60
61
62
63
64
65

1 voltage-gated and ligand-gated channels, TRP and store-operated channels. In general,
2 non-excitabile tissues, including the epithelium, do not express voltage gated Ca^{2+}
3 channels. However, recent studies have shown that T-type Ca^{2+} channels are expressed in
4 cancerous cells, MCF-7 included [48]. MCF-7 cells also express TRPM7 [49] and 8 [50],
5 TRC1 [51] and 6 [52]. TRPV6 is an endothelial calcium entry channel that is strongly
6 expressed in breast adenocarcinoma tissue [7], suggesting that it may play some role in
7 tumor development. Tamoxifen inhibits TRPV6 activity in TRPV6-expressing MCF-7 breast
8 cancer cells [53] and alters Ca^{2+} signalling in MCF-7 breast cancer cells. In malignant
9 glioma cell lines tamoxifen increases cytosolic Ca^{2+} responses to ATP-agonist activation
10 [13]. Some metals (e.g. Pb^{2+} [54] and methyl-mercury [55]), directly block membrane
11 channels leading to a decrease in $[\text{Ca}^{2+}]_i$. $[\text{Pt}(\text{O},\text{O}'\text{-acac})(\gamma\text{-acac})(\text{DMS})]$ reduced the Ca^{2+} -
12 influx from the extracellular space, as demonstrated by the fluorescence quenching due to
13 Mn^{2+} influx (Fig. 2 and 6E). Mn^{2+} enters the cell using Ca^{2+} channels but it is not
14 transported by either the SERCA nor by PMCA. $[\text{Pt}(\text{O},\text{O}'\text{-acac})(\gamma\text{-acac})(\text{DMS})]$ decreases
15 the entry of Mn^{2+} in cells untreated (Fig. 2) and treated with either ATP or thapsigargin (Fig.
16 6E). Since the effects were greatest in ATP-treated cells, it is likely that $[\text{Pt}(\text{O},\text{O}'\text{-acac})(\gamma\text{-acac})(\text{DMS})]$
17 acts also on channels coupled to G proteins or second messengers produced
18 by agonists such as ATP. In this regard, it is known that the PKCs are intracellular
19 transducers also involved in regulating Ca^{2+} influx [30]. PKC- α is the first isoform activated
20 in $[\text{Pt}(\text{O},\text{O}'\text{-acac})(\gamma\text{-acac})(\text{DMS})]$ -treated cells. This activation is temporally compatible with
21 the rapid decrease in the plasmamembrane permeability (Fig. 8A). The involvement of
22 PKC- α is highlighted by the effects elicited by its pharmacological inhibition (Fig. 8B and
23 C). Contrary to other metals, $[\text{Pt}(\text{O},\text{O}'\text{-acac})(\gamma\text{-acac})(\text{DMS})]$ does not interact directly with
24 channels but it activates intracellular signalling leading to the control of some Ca^{2+}
25 channels. We wanted to investigate if the effects of $[\text{Pt}(\text{O},\text{O}'\text{-acac})(\gamma\text{-acac})(\text{DMS})]$ on Ca^{2+}
26 homeostasis also had an impact on the cell ability to handle the complex changes during
27 Ca^{2+} signaling evoked by extracellular stimuli. To this end, we studied the effects of
28 $[\text{Pt}(\text{O},\text{O}'\text{-acac})(\gamma\text{-acac})(\text{DMS})]$ on the strong disturbance in Ca^{2+} levels obtained by
29 stimulating the purinergic receptor. ATP-induced Ca^{2+} response was characterized by two
30 distinct components: an initial rapid and transient rise of $[\text{Ca}^{2+}]_i$, predominantly originating
31 from the endoplasmic reticulum through inositol 1,4,5-trisphosphate receptor (InsP3)
32 receptors (InsP3Rs), and a sustained phase due to Ca^{2+} influx from the extracellular space
33 (Fig. 4A). The latter was previously characterized as extracellular Ca^{2+} entry in response to
34 depletion of the ER Ca^{2+} stores [24,25]. Ca^{2+} ions transients evoked by ATP were
35 effectively reduced by $[\text{Pt}(\text{O},\text{O}'\text{-acac})(\gamma\text{-acac})(\text{DMS})]$, both in the values of the spikes and,
36
37
38
39
40
41
42
43
44
45
46
47
48
49
50
51
52
53
54
55
56
57
58
59
60
61
62
63
64
65

1 especially, in those of the sustained phase of elevated $[Ca^{2+}]_i$ (Fig. 4B). Experiments with
2 La^{3+} , a Ca^{2+} channel blocker that has no effects on PMCA activity, corroborated the idea
3 that the changing in the ATP-provoked $[Ca^{2+}]_i$ profile due to $[Pt(O,O'-acac)(\gamma-acac)(DMS)]$,
4 were due to PMCA activity inhibition and plasma membrane channels closure (Fig. 4B, C
5 and D). The involvement of these channels, and the importance of PMCA inhibition, was
6 observed in experiments performed with ATP in buffer without Ca^{2+} , where $[Pt(O,O'-$
7 $acac)(\gamma-acac)(DMS)]$ increased slightly, but significantly, the ATP-provoked Ca^{2+} transient
8 (Fig. 5A and C). This increase may be due to the inhibition of PMCA. We noticed that the
9 addition of external Ca^{2+} causes a significant extracellular Ca^{2+} entry that is in part blocked
10 by $[Pt(O,O'-acac)(\gamma-acac)(DMS)]$ (Figs. 5 and 6). $[Pt(O,O'-acac)(\gamma-acac)(DMS)]$ does not
11 seem to affect the Ca^{2+} released from the intracellular stores because no significant effect
12 on Ca^{2+} transient provoked by ATP was evident in cells with the InsP3Rs blocked by 2-APB
13 (with the exception of a slight increase in the plateau). This may also be due to the
14 decreased PMCA activity (Fig. 5B and C). Consistently, $[Pt(O,O'-acac)(\gamma-acac)(DMS)]$ had
15 effect on Ca^{2+} peak provoked by ATP in Ca^{2+} -free buffers and on the $[Ca^{2+}]_i$ returning to
16 control values, a phase that resulted to be slower due to reduced calcium efflux (Fig. 6B
17 and C). Finally, it is important to note that the results we obtained (Tab. I) on the various
18 breast cell lines provide evidence that $[Pt(O,O'-acac)(\gamma-acac)(DMS)]$ may be a promising
19 new anticancer agent, as it exhibited higher calcium homeostasis perturbation in cancer
20 cell lines than in non-cancerous MCF-10A cells, which also appeared to be less sensitive
21 to the cytotoxic effect of the Pt-compound [16].

22 In conclusion, we demonstrated that $[Pt(O,O'-acac)(\gamma-acac)(DMS)]$ alters the $[Ca^{2+}]_i$ and
23 that this change is due both to the PKC- α -mediated closure of some channels and to the
24 inhibition of PMCA. The key points of this model are summarized in Fig. 10. The overall
25 effect of $[Pt(O,O'-acac)(\gamma-acac)(DMS)]$ is to increase the $[Ca^{2+}]_i$, an effect that is linked to
26 its ability to trigger rapid apoptosis in MCF-7 cells.

27 **Conflict of interest**

28 The authors state no conflict of interest.

29 **Acknowledgements**

30 The research was supported by University of Salento (Fondi di Ateneo per la Ricerca di
31 Base, 2009).

References

- 1
2 [1] Carafoli E, Santella L, Branca D, Brini M. Generation, control, and processing
3 of cellular calcium signals. *Crit Rev Biochem Mol Biol* 2001;36:107-260.
4
5
6
7 [2] Lipskaia L, Lompré AM. Alteration in temporal kinetics of Ca^{2+} signaling and
8 control of growth and proliferation. *Biol Cell* 2004;96:55–68.
9
10
11
12 [3] Kahl CR, Means AR. Regulation of cell cycle progression by
13 calcium/calmodulin-dependent pathways. *Endocr Rev* 2003;24:719–736.
14
15
16
17
18 [4] Orrenius S, Zhivotovsky B, Nicotera P. Regulation of cell death: the calcium-
19 apoptosis link. *Nat Rev Mol Cell Biol* 2003; 4:552–565.
20
21
22
23 [5] Berridge MJ, Bootman MD, Roderick HL. Calcium signalling: dynamics,
24 homeostasis and remodelling. *Nat Rev Mol Cell Biol* 2003;4:517-529.
25
26
27
28
29 [6] Rizzuto R, Pozzan T. When calcium goes wrong: genetic alterations of a
30 ubiquitous signaling route. *Nat Genet* 2003; 34:135–141.
31
32
33
34 [7] Zhuang L, Peng JB, Tou L, Takanaga H, Adam RM, Hediger Ma et al. Calcium-
35 selective ion channel, CaT1, is apically localized in gastrointestinal tract epithelia
36 and is aberrantly expressed in human malignancies. *Lab Invest* 2002;82:1755–
37 1764.
38
39
40
41
42
43 [8] Kamrava MR, Michener CM, Kohn EC. Calcium signaling as a molecular target
44 in cancer. *Pharmaceutical News* 2002;9:435–42.
45
46
47
48
49 [9] Lee WJ, Roberts-Thomson SJ, Holman NA, May FJ, Lehrbach GM, Monteith
50 GR. Expression of plasma membrane calcium pump isoform mRNAs in breast
51 cancer cell lines. *Cell Signal* 2002;14:1015–1022.
52
53
54
55
56 [10] Reisner PD, Brandt PC, Vanaman TC. Analysis of plasma membrane Ca^{2+} -
57 ATPase expression in control and SV40-transformed human fibroblasts. *Cell*
58 *Calcium* 1997;21:53–62.
59
60
61
62
63
64
65

- 1
2
3
4
5
6
7
8
9
10
11
12
13
14
15
16
17
18
19
20
21
22
23
24
25
26
27
28
29
30
31
32
33
34
35
36
37
38
39
40
41
42
43
44
45
46
47
48
49
50
51
52
53
54
55
56
57
58
59
60
61
62
63
64
65
- [11] Chene P. ATPases as drug targets: learning from their structure. *Nat Rev Drug Discov* 2002;1:665–673.
- [12] Johnson PH, Walker RP, Jones SW, Stephens K, Meurer J, Zajchowski, et al. Multiplex gene expression analysis for high-throughput drug discovery: screening and analysis of compounds affecting genes overexpressed in cancer cells. *Mol Cancer Ther* 2002;1:1293–1304.
- [13] Zhang W, Couldwell WT, Song H, Takano T, Lin JHC, et al. Tamoxifen-induced Enhancement of Calcium Signaling in Glioma and MCF-7 Breast Cancer Cells. *Cancer Res* 2000;60:5395–5400.
- [14] De Pascali SA, Papadia P, Ciccarese A, Pacifico C, Fanizzi FP. First examples of β -diketonate platinum II complexes with sulfoxide ligands. *Eur J Inorg Chem* 2005;5:788–796.
- [15] Muscella A, Calabriso N, De Pascali SA, Urso L, Ciccarese A, Fanizzi FP, et al. New platinum II complexes containing both an O,O'-chelated acetylacetonate ligand and a sulfur ligand in the platinum coordination sphere induce apoptosis in HeLa cervical carcinoma cells. *Biochem Pharmacol* 2007;74:28–40.
- [16] Muscella A, Calabriso N, Fanizzi FP, De Pascali SA, Urso L, Ciccarese A, et al. [Pt O,O'-acac γ -acac DMS], a new Pt compound exerting fast cytotoxicity in MCF-7 breast cancer cells via the mitochondrial apoptotic pathway. *Br J Pharmacol* 2008;153:34–49.
- [17] Grynkiewicz G, Poenie M, Tsien RY. A new generation of calcium indicators with greatly improved fluorescence properties. *J Biol Chem* 1985;260:3440–3450.
- [18] Higgins JA. Separation and analysis of membrane lipid components. In: JBC Findlay & WH Evans editors. *In Biological Membranes, a Practical Approach*. Oxford: IRL Press; 1987. p. 103–137.

- 1
2
3
4
5
6
7
8
9
10
11
12
13
14
15
16
17
18
19
20
21
22
23
24
25
26
27
28
29
30
31
32
33
34
35
36
37
38
39
40
41
42
43
44
45
46
47
48
49
50
51
52
53
54
55
56
57
58
59
60
61
62
63
64
65
- [19] Lytton J, Westlin M, Hanley MR. Thapsigargin inhibits the sarcoplasmic and endoplasmic reticulum Ca^{2+} -ATPase family of calcium pumps. *J Biol Chem* 1991;266:17067–17071.
- [20] Sepúlveda MR, Berrocal M, Marcos D, Wuytack F, Mata AM. Functional and immunocytochemical evidence for the expression and localization of the secretory pathway Ca^{2+} -ATPase isoform 1 SPCA1 in cerebellum relative to other Ca^{2+} pumps. *J Neurochem* 2007;103:1009–18.
- [21] Gatto C, Hale CC, Xu W, Milanick MA. Eosin, a potent inhibitor of the plasma membrane Ca pump, does not inhibit the cardiac Na-Ca exchanger. *Biochemistry* 1995;34:965–972.
- [22] Muscella A, Calabriso N, Vetrugno C, Urso L, Fanizzi FP, De Pascali SA et al. Sublethal concentrations of the platinum II complex [Pt O,O'-acac Y-acac DMS] alter the motility and induce anoikis in MCF-7 cells. *Br J Pharmacol* 2010: in press.
- [23] Merritt JE, Hallam TJ. Platelets and parotid acinar cells have different mechanisms for agonist-stimulated divalent cation entry. *J Biol Chem* 1998;263:6161–4.
- [24] Muscella A, Greco S, Elia MG, Storelli C, Marsigliante S. Angiotensin II stimulation of Na^+/K^+ -ATPase activity and cell growth by calcium-independent pathway in MCF-7 breast cancer cells. *J Endocrinol* 2002;173:315–323.
- [25] Bowler WB, Dixon CJ, Halleux C, Maier R, Bilbe G, Fraser WD, et al. Signalling in human osteoblasts by extracellular nucleotides-their weak induction of the c-Fos proto-oncogene via Ca^{2+} mobilisation is strongly potentiated by a parathyroid hormone/cAMP-dependent protein kinase pathway independently of mitogen-activated protein kinase. *J Biol Chem* 1999;274:14315-14324.
- [26] Rossi AM, Picotto G, de Boland AR, Boland RL. Evidence on the operation of ATP-induced capacitative calcium entry in breast cancer cells and its blockade by 17beta-estradiol. *J Cell Biochem* 2002;87:324–33.

- 1
2
3
4
5
6
7
8
9
10
11
12
13
14
15
16
17
18
19
20
21
22
23
24
25
26
27
28
29
30
31
32
33
34
35
36
37
38
39
40
41
42
43
44
45
46
47
48
49
50
51
52
53
54
55
56
57
58
59
60
61
62
63
64
65
- [27] Maruyama T, Kanaji T, Nakade S, Kanno T, Mikoshiba K. 2APB, 2-aminoethoxydiphenyl borate, a membrane-penetrable modulator of Ins 1,4,5 P₃-induced Ca²⁺ release. *J Biochem* 1997;122:498–505.
- [28] Peppiatt CM, Collins TJ, Mackenzie L, Conway SJ, Holmes AB, Bootman MD, et al. 2-Aminoethoxydiphenyl borate 2-APB antagonises inositol 1,4,5-trisphosphate-induced calcium release, inhibits calcium pumps and has a use-dependent and slowly reversible action on store-operated calcium entry channels. *Cell Calcium* 2003;34:97–108.
- [29] Anantamongkol U, Takemura H, Suthiphongchai T, Krishnamra N, Horio Y. Regulation of Ca²⁺ mobilization by prolactin in mammary gland cells: possible role of secretory pathway Ca²⁺-ATPase type 2. *Biochem Biophys Res Comm* 2007;352:537–542.
- [30] McHugh D, Sharp EM, Scheuer T, Catterall WA . Inhibition of cardiac L-type calcium channels by protein kinase C phosphorylation of two sites in the N-terminal domain. *Proc Natl Acad Sci U S A* 2000;97:12334–8.
- [31] Muscella A, Greco S, Elia MG, Storelli C, Marsigliante S. PKC-zeta is required for angiotensin II-induced activation of ERK and synthesis of C-FOS in MCF-7 cells. *J Cell Physiol* 2003;197:61–8.
- [32] Qatsha KA, Rudolph C, Marme D, Schachtele C, May WS. Gö 6976, a selective inhibitor of protein kinase C, is a potent antagonist of human immunodeficiency virus 1 induction from latent/low-level-producing reservoir cells in vitro. *Proc Natl Acad Sci USA* 1993;90:4674–4678.
- [33] Osborne CK, Yochmowitz MG, Knight WA 3rd, McGuire WL. The value of estrogen and progesterone receptors in the treatment of breast cancer. *Cancer* 1980;46:2884–2888.
- [34] Thorpe SM. Estrogen and progesterone receptor determinations in breast cancer, technology, biology and clinical significance. *Acta Oncol* 1988;27:1–19.

- 1
2
3
4
5
6
7
8
9
10
11
12
13
14
15
16
17
18
19
20
21
22
23
24
25
26
27
28
29
30
31
32
33
34
35
36
37
38
39
40
41
42
43
44
45
46
47
48
49
50
51
52
53
54
55
56
57
58
59
60
61
62
63
64
65
- [35] Wei MC, Zong WX, Cheng EH, Lindsten T, Panoutsakopoulou V, Ross AJ, et al. Proapoptotic BAX and BAK: a requisite gateway to mitochondrial dysfunction and death. *Science* 2001;292:727–730.
- [36] Florea AM, Büsselberg D. Occurrence, use and potential toxic effects of metals and metal compounds. *Biometals* 2006;19:419–427.
- [37] Tomaszewski, Büsselberg D. SnCl₂ reduces voltage-activated calcium channel currents of dorsal root ganglion neurons of rats. *Neurotoxicology* 2008;29:958–963.
- [38] Kawai Y, Nakao T, Kunimura N, Kohda Y, Gemba M. Relationship of intracellular calcium and oxygen radicals to cisplatin-related renal cell injury. *J Pharmacol Sci* 2006;100:65–72.
- [39] Lee W, Robinson J A, Holman NA, McCall MN, Roberts-Thomson SJ, Monteith GR . Antisense-mediated Inhibition of the Plasma Membrane Calcium-ATPase Suppresses Proliferation of MCF-7 Cells. *J Biol Chem* 2005;280:27076–27084.
- [40] Pariente JA, Camello C, Camello PJ, Salido GM. Release of calcium from mitochondrial and non mitochondrial intracellular stores in mouse pancreatic acinar cells by hydrogen peroxide. *J Membr Biol* 2001;179:27–35.
- [41] Zaidi A, Michaelis ML. Effects of reactive oxygen species on brain synaptic plasma membrane Ca²⁺-ATPase. *Free Radic Biol Med* 1999;27:810–821.
- [42] Bruce JIE, Elliott AC. Oxidant-impaired intracellular Ca²⁺ signaling in pancreatic acinar cells: role of the plasma membrane Ca²⁺-ATPase. *Am J Physiol Cell Physiol* 2007;293:C938–C950.
- [43] Fariss MW, Chan CB, Patel M, Van Houten B, Orrenius S. Role of mitochondria in toxic oxidative stress. *Mol Interv* 2005;5:94–111.
- [44] Pászty K, Antalffy G, Hegedüs L, Padányi R, Penheiter AR, Filoteo AG et al. Cleavage of the plasma membrane Ca²⁺ ATPase during apoptosis. *Ann N Y Acad*

Sci. 2007;1099:440–50.

- 1
2
3
4
5
6
7
8
9
10
11
12
13
14
15
16
17
18
19
20
21
22
23
24
25
26
27
28
29
30
31
32
33
34
35
36
37
38
39
40
41
42
43
44
45
46
47
48
49
50
51
52
53
54
55
56
57
58
59
60
61
62
63
64
65
- [45] Schwab BL, Guerini D, Didszun C, Bano D, Ferrando-May E, Fava E et al. Cleavage of plasma membrane calcium pumps by caspases: a link between apoptosis and necrosis. *Cell Death Differ* 2002;9:818–831.
- [46] Bano D, Young KW, Guerin CJ, Lefevre R, Rothwell NJ, Naldini L, et al. Cleavage of the plasma membrane $\text{Na}^+/\text{Ca}^{2+}$ exchanger in excitotoxicity. *Cell* 2005; 120:275–285.
- [47] Clapham DE. Calcium signaling. *Cell* 2007;131: 1047–1058.
- [48] Taylor JT, Huang L, Pottle JE, Liu K, Yang Y, Zeng X et al. Selective blockade of T-type Ca^{2+} channels suppresses human breast cancer cell proliferation. *Cancer Lett* 2008;267:116-24.
- [49] Guilbert A, Gautier M, Dhennin-Duthille I, Haren N, Sevestre H, Ouadid-Ahidouch H. Evidence that TRPM7 is required for breast cancer cell proliferation. *Am J Physiol Cell Physiol* 2009;297:493-502.
- [50] Chodon D, Guilbert A, Dhennin-Duthille I, Gautier M, Telliez MS, Sevestre H, Ouadid-Ahidouch H. Estrogen regulation of TRPM8 expression in breast cancer cells. *BMC Cancer* 2010;10:212-219.
- [51] El Hiani Y, Ahidouch A, Lehen'kyi V, Hague F, Gouilleux F, Mentaverri R et al. Extracellular Signal-Regulated Kinases 1 and 2 and TRPC1 Channels are Required for Calcium- Sensing Receptor-Stimulated MCF-7 Breast Cancer Cell Proliferation. *Cell Physiol Biochem* 2009;23:335-346.
- [52] Guilbert A, Dhennin-Duthille I, Hiani YE, Haren N, Khorsi H, Sevestre H, et al. Expression of TRPC6 channels in human epithelial breast cancer cells. *BMC Cancer* 2008;8:125-129.

- 1
2
3
4
5
6
7
8
9
10
11
12
13
14
15
16
17
18
19
20
21
22
23
24
25
26
27
28
29
30
31
32
33
34
35
36
37
38
39
40
41
42
43
44
45
46
47
48
49
50
51
52
53
54
55
56
57
58
59
60
61
62
63
64
65
- [53] Bolanz KA, Kovacs GG, Landowski CP, Hediger MA. Tamoxifen inhibits TRPV6 activity via estrogen receptor-independent pathways in TRPV6-expressing MCF-7 breast cancer cells. *Mol Cancer Res.* 2009;7:2000-10.
- [54] Büsselberg D. Actions of metals on membrane channels, calcium homeostasis and synaptic plasticity. In: AV Hirner and H Emons, editors. *Organometal and Metalloid Specism in the Environment: Analysis, Distribution, Processes and Toxicological Evaluation.* Springer, Wien, New York; 2004. p. 259–281.
- [55] Leonhardt R, Pekel M, Platt B, Haas HL, Busselberg D. Voltage-activated calcium channel currents of rat DRG neurons are reduced by mercuric chloride HgCl_2 and methylmercury CH_3HgCl . *Neurotoxicology* 1996;17:85–92.

LEGENDS TO FIGURES

Fig. 1. Effects of Pt(II) compounds on $[Ca^{2+}]_i$.

Intracellular Ca^{2+} concentration was quantified by fluorescence after loading the cells with the calcium indicator fura-2-AM. Time-course of the effects of various concentrations of (A) $[Pt(O,O'-acac)(\gamma-acac)(DMS)]$, (B) Cisplatin and (C) 100 μM Carboplatin on $[Ca^{2+}]_i$ in MCF-7 cells. Results shown are representative of six separate experiments. Values with shared letters are not significantly different according to Bonferroni/Dunn post hoc tests.

Fig. 2. Comparison of the permeabilities of the plasma membrane to Mn^{2+} in absence and in presence of $[Pt(O,O'-acac)(\gamma-acac)(DMS)]$.

Mn^{2+} entry was measured by the quenching of fluorescence with an excitation wavelength of 360 nm, and an emission wavelength of 510 nm. The curves represent fluorescence relative to total quenching attained by the addition of digitonin to saturate fura-2 with Mn^{2+} . (A) Cells were kept in nominally Ca^{2+} -free medium, as 2 mM Mn^{2+} was applied to the medium (arrow), it entered cells, with Mn^{2+} entry much slower in $[Pt(O,O'-acac)(\gamma-acac)(DMS)]$ -treated cells. Mn^{2+} entry was blocked by the impermeant cation La^{3+} (100 μM), and $[Pt(O,O'-acac)(\gamma-acac)(DMS)]$ had, on Mn^{2+} influx, effects similar to those obtained by La^{3+} . Each tracing is representative of five separate experiments. (B) The permeability of MCF-7 cell plasma membrane was significantly decreased by $[Pt(O,O'-acac)(\gamma-acac)(DMS)]$ in a dose-dependent manner. Mn^{2+} entry in cells treated with 10 μM $[Pt(O,O'-acac)(\gamma-acac)(DMS)]$ was the same in the presence or in the absence of La^{3+} . Average data are from experiments shown in A (n=5). Values with shared letters are not significantly different according to Bonferroni/Dunn post hoc tests. $Pt(acac)_2DMS$ stands for $Pt(O,O'-acac)(\gamma-acac)DMS$.

Fig. 3. Effects of $[Pt(O,O'-acac)(\gamma-acac)(DMS)]$ on Ca^{2+} -ATPases activities.

(A) ATPase activity was assessed in the presence of 0.5 mM ouabain, as inorganic phosphate (Pi) liberated from ATP during a 10 min incubation at 37°C. Ca^{2+} refers to incubation in the presence of 80 μM $CaCl_2$, while EGTA refers to incubation with 800 μM EGTA. Ca^{2+} -sensitive ATPase activity is the difference between the two conditions. In order to identify the relative contributions of the PMCA, SPCA and SERCA, Ca^{2+} -sensitive ATPase activity was assessed in the presence of the SERCA inhibitor thapsigargin or/and in presence of eosin and orthovanadate, as detailed in "Material and Method". The Ca^{2+} -ATPase activities were expressed as μM of Pi liberated per mg of protein per hour, based

on values from a standard curve of the absorbance using various concentrations of free Pi.

(B) MCF-7 cells were stimulated or not with 0.5 or 10 μM [Pt(O,O'-acac)(γ -acac)(DMS)] for 10 min, and then SERCA and PMCA activities were assessed.

(C) Effects of increasing incubation times of 10 μM [Pt(O,O'-acac)(γ -acac)(DMS)] on PMCA activity in MCF-7 cells.

(D) MCF-7 were stimulated with ATP (100 μM) for 2.5 min; afterwards, [Pt(O,O'-acac)(γ -acac)(DMS)] (10 μM) was added for the indicated times in order to assess its effects on the effects induced by ATP on the PMCA activity. The data are means \pm S.D. of four different experiments run in triplicate. Values with shared letters are not significantly different according to Bonferroni/Dunn post hoc tests. Pt(acac)₂DMS stands for Pt(O,O'-acac)(γ -acac)DMS.

Fig. 4. Effects of [Pt(O,O'-acac)(γ -acac)(DMS)] and La³⁺ on the ATP-induced Ca²⁺ transients.

(A) MCF-7 cells, loaded with fura-2-AM, were stimulated with 100 μM ATP in the presence of extracellular Ca²⁺. The effects of ATP on [Ca²⁺]_i were also assessed in the presence of increasing concentrations of [Pt(O,O'-acac)(γ -acac)(DMS)]. Each tracing is representative of seven separate experiments.

(B) Inhibitory action of [Pt(O,O'-acac)(γ -acac)(DMS)] on ATP-induced [Ca²⁺]_i transients was quantified by the *b/a* ratio, in which *a* represents the maximum peak amplitude (see *B, inset*) and *b* is the amplitude of the sustained component evaluated after 2 min from ATP administration. The *b/a* ratio was calculated for [Pt(O,O'-acac)(γ -acac)(DMS)], and for 100 μM La³⁺, and then plotted for the various concentrations of [Pt(O,O'-acac)(γ -acac)(DMS)]. Each bar represents mean \pm S.D. of seven separate experiments. Values with shared letters are not significantly different according to Bonferroni/Dunn post hoc tests.

(C) Effect of lanthanum on ATP-mediated [Ca²⁺]_i increases in MCF-7 cells; cells were incubated with 100 μM ATP or pre-treated with 100 μM La³⁺ for 30 sec prior stimulation with 100 μM ATP. Each tracing is representative of seven separate experiments.

(D) The rate of decline of [Ca²⁺]_i transient assayed in a time interval of 1 min after the peak, is a relative measure of PMCA-mediated free intracellular Ca²⁺ efflux. The rates of decline in [Ca²⁺]_i obtained with the various [Pt(O,O'-acac)(γ -acac)(DMS)] concentrations and with 100 μM La³⁺ were plotted against the relative [Ca²⁺]_i peak values for comparisons of PMCA-mediated Ca²⁺ efflux rates in [Pt(O,O'-acac)(γ -acac)(DMS)]-treated and non MCF-7 cells. Pt(acac)₂DMS stands for Pt(O,O'-acac)(γ -acac)DMS.

Fig. 5. Effect of 2-aminoethoxydiphenyl borate (2-APB) on ATP- and ATP plus [Pt(O,O'-acac)(γ-acac)(DMS)]-induced intracellular Ca²⁺ release and extracellular Ca²⁺ entry.

(A, B) 2-APB (20 μM), a membrane-permeant InsP3R blocker, was applied to MCF-7, kept in nominal Ca²⁺-free medium, 10 min before the stimulation with 100 μM ATP (A) or the co-stimulation with ATP and 10 μM [Pt(O,O'-acac)(γ-acac)(DMS)] (B). 2-APB caused a significant inhibition of the ATP-induced intracellular Ca²⁺ release both in the absence and in the presence of 10 μM [Pt(O,O'-acac)(γ-acac)(DMS)]. Afterwards, 2 mM CaCl₂ was added in order to assess the extracellular Ca²⁺ entry. Example traces of [Ca²⁺]_i induced transients are shown.

(C, D) Summary of the effects of 2-APB on ATP- and ATP+[Pt(O,O'-acac)(γ-acac)(DMS)]-induced Ca²⁺ release (C) and extracellular Ca²⁺ entry (D). Data are presented as average percentages ± S.D. of control (ATP, open bar; [Pt(O,O'-acac)(γ-acac)(DMS)], solid bar), i.e., the amplitude of the Ca²⁺ peak (C) and of extracellular Ca²⁺ entry (D) measured in the absence of 2-APB. The data are means ± S.D. of five different experiments. Values with shared letters are not significantly different according to Bonferroni/Dunn post hoc tests. Pt(acac)₂DMS stands for [Pt(O,O'-acac)(γ-acac)DMS].

Fig. 6. Effect of [Pt(O,O'-acac)(γ-acac)(DMS)] on extracellular Ca²⁺ entry.

(A) Intracellular Ca²⁺ stores were previously depleted by exposure to 1 μM thapsigargin (TG) in Ca²⁺-free solution and then 2 mM CaCl₂ was added. Extracellular Ca²⁺ entry into MCF-7 cells was evaluated in the absence and in the presence of 10 μM [Pt(O,O'-acac)(γ-acac)(DMS)] or 2 μM orthovanadate ([VO₃(OH)]₂).

(B) Effect of 10 μM [Pt(O,O'-acac)(γ-acac)(DMS)] on the extracellular Ca²⁺ entry into MCF-7 cells stimulated with ATP. In nominal Ca²⁺-free medium, 100 μM ATP was added followed by 2 mM CaCl₂ after 4 min in the absence and in the presence of 10 μM [Pt(O,O'-acac)(γ-acac)(DMS)].

(C, D) [Ca²⁺]_i values obtained from A and B representing the mobilization of internal calcium (peak in C) and the extracellular Ca²⁺ entry (CaCl₂) after 6.5 min (in D) of stimulation with ATP or thapsigargin in the presence or absence of [Pt(O,O'-acac)(γ-acac)(DMS)]. The data are means ± S.D. of four different experiments run in triplicate. Values with shared letters are not significantly different according to Bonferroni/Dunn post hoc tests. Pt(acac)₂DMS stands for [Pt(O,O'-acac)(γ-acac)DMS].

(E) Effect of 10 μM [Pt(O,O'-acac)(γ-acac)(DMS)] on thapsigargin- or ATP-induced extracellular Mn²⁺ entry in Ca²⁺-free solution. After Ca²⁺ store depletion with thapsigargin

or ATP, cells were exposed to 2 mM Mn^{2+} , in the presence or in the absence of [Pt(O,O'-acac)(γ -acac)(DMS)]. Each tracing is representative of five separate experiments.

(F) Average data are from experiments shown in (E) (n=5). Values with shared letters are not significantly different according to Bonferroni/Dunn post hoc tests.

Fig. 7. Effects of [Pt(O,O'-acac)(γ -acac)(DMS)] on Na^+/Ca^{2+} -Exchanger activity

(A) Ca^{2+} influx in cells stimulated with ATP, in buffers with Na^+ concentrations of 0 and 140 nM, in the presence (B) or not (A) of [Pt(O,O'-acac)(γ -acac)(DMS)]. Results shown are representative of four experiments.

(C) $\Delta[Ca^{2+}]_i$ values obtained from A and B after 30 sec (peak) stimulation with ATP in normal and Na^+ -free buffers in the presence or not of [Pt(O,O'-acac)(γ -acac)(DMS)].

The data are means \pm S.D. of four different experiments run in triplicate. Values with shared letters are not significantly different according to Bonferroni/Dunn post hoc tests. Pt(acac)₂DMS stands for [Pt(O,O'-acac)(γ -acac)DMS].

Fig. 8. The effect of [Pt(O,O'-acac)(γ -acac)(DMS)] on extracellular Ca^{2+} entry is due to PKC- α activation

(A) MCF-7 cells were treated without or with 10 μ M [Pt(O,O'-acac)(γ -acac)(DMS)] for the indicated times. Cytosol (cyt) and membrane (mem) fractions for translocation studies, were analyzed by western blotting with specific anti-PKCs antibodies. The purity of fractions was tested by immunoblotting with anti β -actin and anti- α subunit of Na^+/K^+ ATPase monoclonal antibodies. The figures are representative of four independent experiments.

(B, C) MCF-7 cells, loaded with fura-2-AM, and kept in nominally Ca^{2+} -free medium, were stimulated with ATP or ATP plus 10 μ M [Pt(O,O'-acac)(γ -acac)(DMS)], with or without 1 μ M Gö 6976. (C) Mn^{2+} entry was measured by the quenching of fluorescence with an excitation wavelength of 360 nm, and an emission wavelength of 510 nm. The curves represent fluorescence relative to total quenching attained by the addition of digitonin to saturate fura-2 with Mn^{2+} . Each tracing is representative of six separate experiments.

Arrows indicate time points at which 100 μ M ATP, 2 mM $CaCl_2$ or 2 mM Mn^{2+} were added. Pt(acac)₂DMS stands for [Pt(O,O'-acac)(γ -acac)DMS].

Fig. 9. The effect of [Pt(O,O'-acac)(γ -acac)(DMS)] on PMCA is due to Reactive Oxygen Species (ROS) generation.

(A) Cells were treated or not with 10 μ M [Pt(O,O'-acac)(γ -acac)(DMS)] for the indicated

time intervals. ROS production was assayed by NBT reduction as described in “Material and Methods.” The data are means \pm S.D. of four different experiments. Values with shared letters are not significantly different according to Bonferroni/Dunn post hoc tests.

(B) Cells were treated or not with 10 μ M [Pt(O,O'-acac)(γ -acac)(DMS)] and with or without apocyanin for 20 min and superoxide anion production was determined by MitoSOX staining in fluorescence microscopy. Lower panel shows the increase in superoxide production induced by [Pt(O,O'-acac)(γ -acac)(DMS)] by fluorescence microscopy. The mean fluorescence intensities (MFI/cell) \pm S.D. are shown in upper panel (n= 4; * p \leq 0.001).

(C) Time-response experiments with 10 μ M [Pt(O,O'-acac)(γ -acac)(DMS)] showing the increase of MitoSOX Red fluorescence induced by [Pt(O,O'-acac)(γ -acac)(DMS)]. Results are expressed in MFI/cell \pm S.D. of four different experiments.

(D, E) Cells preincubated with or without apocynin (Apo) or diphenyleneiodonium (DPI) for 30 min were exposed to 10 μ M [Pt(O,O'-acac)(γ -acac)(DMS)] for 10 min. ROS production and PMCA activity were assayed as described in “Material and Methods.” The data are means \pm S.D. of four different experiments. Values with shared letters are not significantly different according to Bonferroni/Dunn post hoc tests. Pt(acac)₂DMS stands for [Pt(O,O'-acac)(γ -acac)DMS].

Fig. 10. Mechanisms of Pt(O,O'-acac)(γ -acac)(DMS)]-induced apoptosis.

Pt(O,O'-acac)(γ -acac)(DMS)] alters the [Ca²⁺]_i; this change is due both to the PKC- α -mediated closure of some channels and, primarily, to the decrease of PMCA activity, due to NADPH oxidase and mitochondrial ROS production.

Previous results [16] demonstrated that Pt(O,O'-acac)(γ -acac)(DMS)] targets the mitochondria, resulting in dissipation of the membrane potential that may minimize the contribution of mitochondria to Ca²⁺ homeostasis. Subsequent mitochondrial release of cyt c leads to activation of caspase-9, resulting in apoptosis. Pt(O,O'-acac)(γ -acac)(DMS)] also decreased Bcl-2 expression thus diminishing its contribution to the endoplasmic reticulum Ca²⁺ uptake, an effect likely related to its anti-apoptotic function.

Tab. I Effects of Pt(O,O'-acac)(γ -acac)(DMS)] in human breast cell lines

Δ [Ca²⁺]_i represents the increase in free intracellular calcium concentration, obtained by fluorimetry using Fura-2, in cell incubated with 10 μ M Pt(O,O'-acac)(γ -acac)(DMS)] for 20 min.

Δ F360min⁻¹ represents the decrease of the plasma membrane permeability to Mn²⁺ influx

after the addition of 10 μM [Pt(O,O'-acac)(γ -acac)(DMS)].

ΔPMCA represents the decrease in the ATPase activity of the PMCA in cells incubated with 10 μM Pt(O,O'-acac)(γ -acac)(DMS)] for 10 min.

ΔNBT represent the increase in ROS generation obtained by nitroblue tetrazolium (NBT) assay in cells incubated with 10 μM Pt(O,O'-acac)(γ -acac)(DMS)] for 10 min.

Results are expressed as the percentage ratio over control cells. The data are means \pm S.D. of four different experiments. Values with shared letters are not significantly different according to Bonferroni/Dunn post hoc tests.

Accepted Manuscript

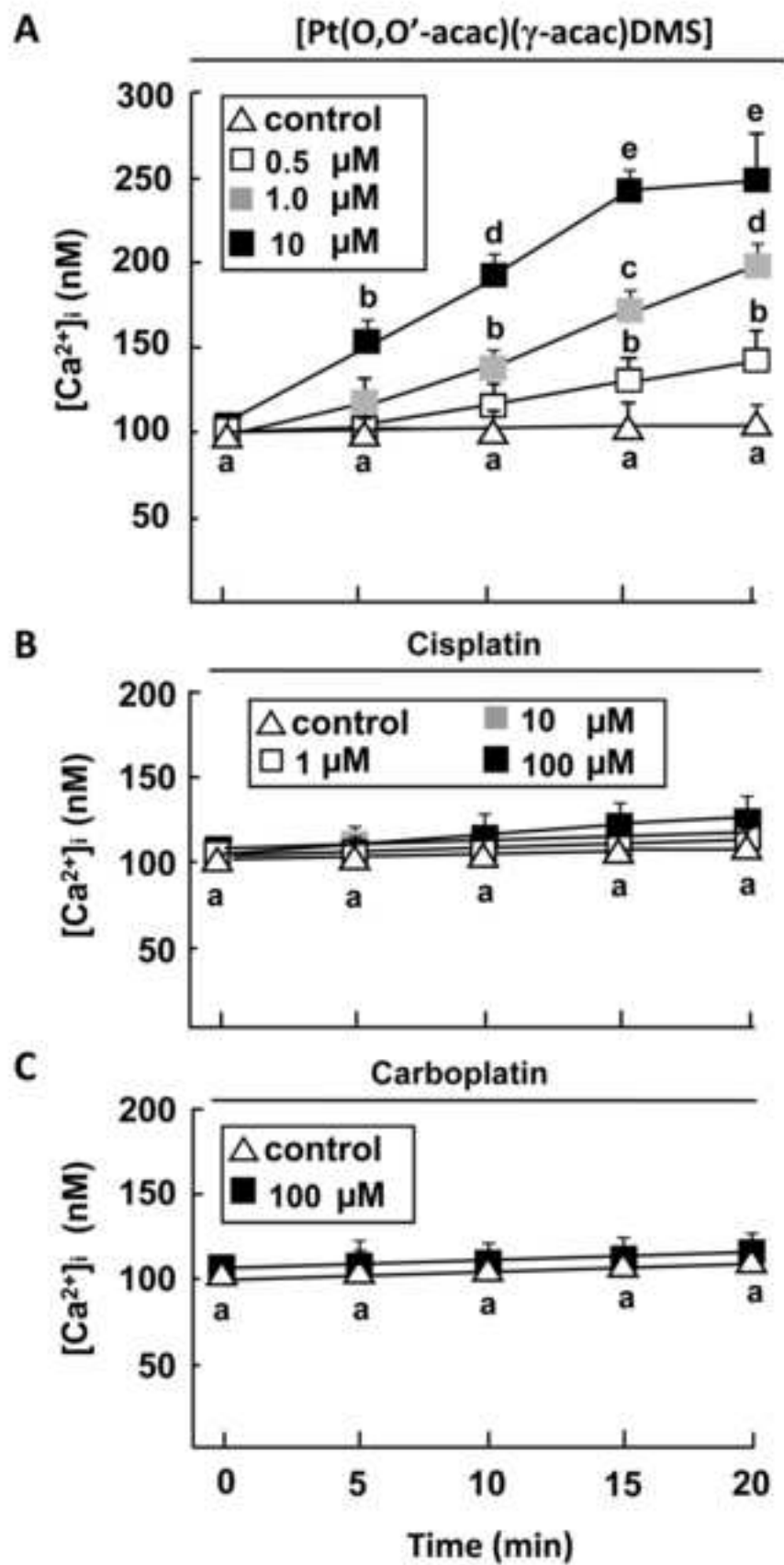
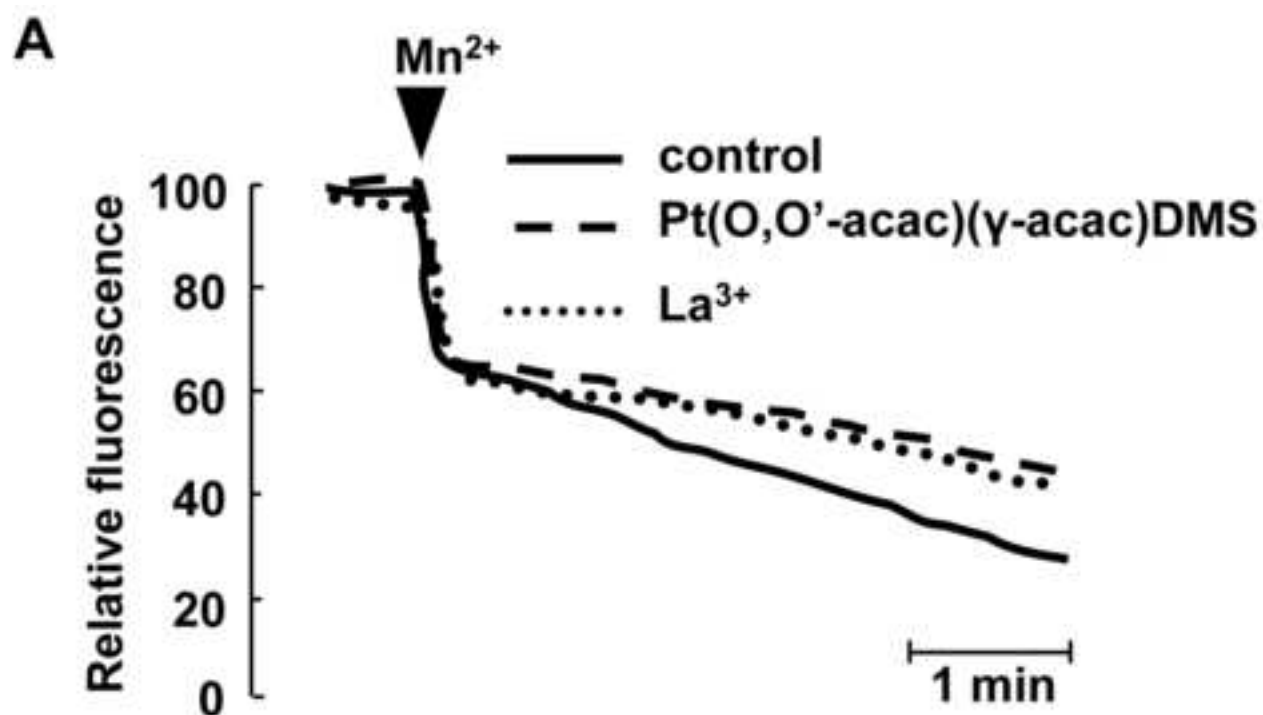


FIG.1



B

	$\Delta F_{360} \cdot \text{min}^{-1}$
Control	6.83 ± 0.32^a
0.5 μM Pt(O,O'-acac)(γ-acac)DMS	4.79 ± 0.27^b
1.0 μM Pt(O,O'-acac)(γ-acac)DMS	3.95 ± 0.24^c
10 μM Pt(O,O'-acac)(γ-acac)DMS	2.19 ± 0.13^d
100 μM La ³⁺	2.22 ± 0.19^d
100 μM La ³⁺ + 10 μM Pt(acac) ₂ DMS	2.16 ± 0.10^d

FIG. 2

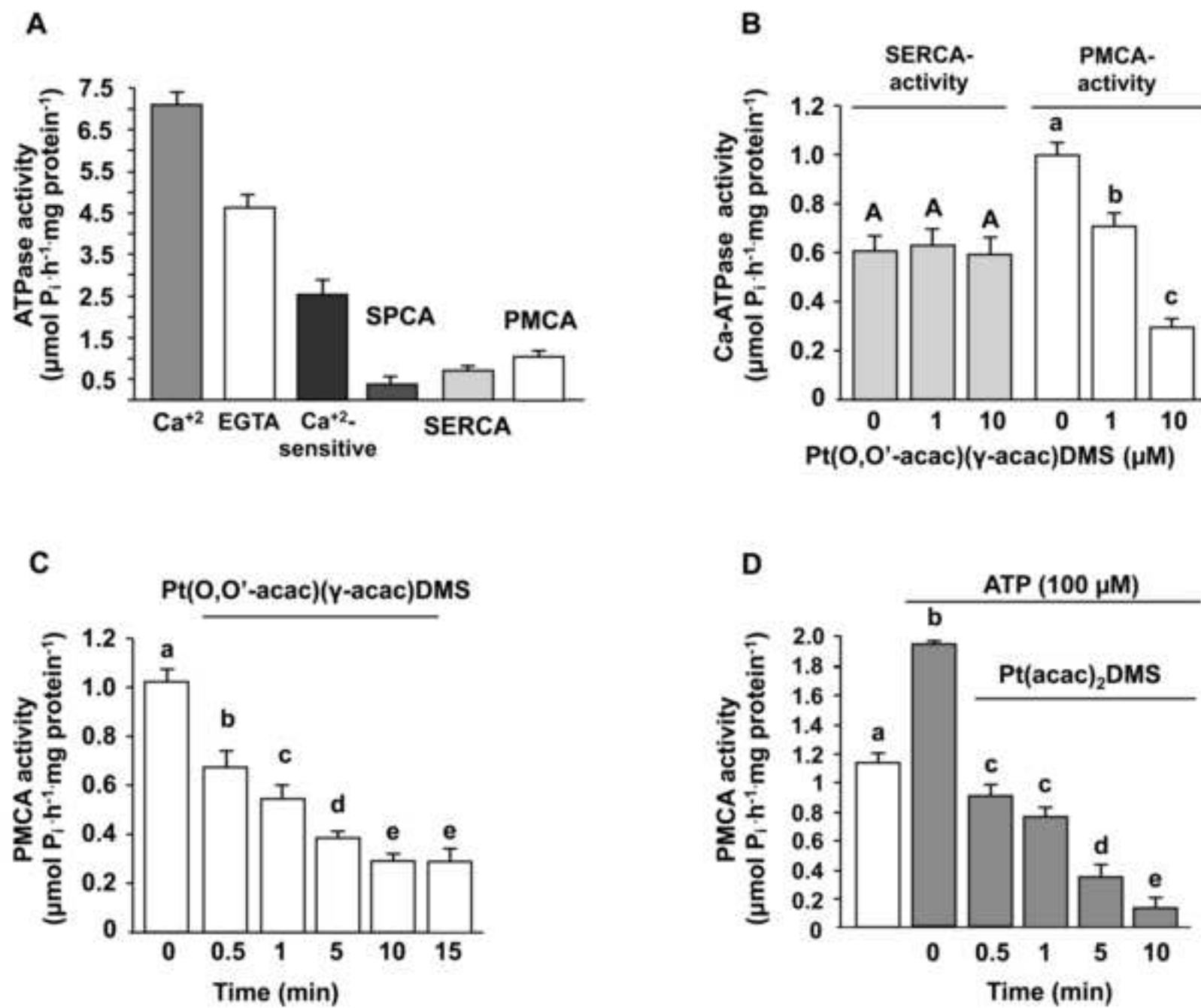


FIG. 3

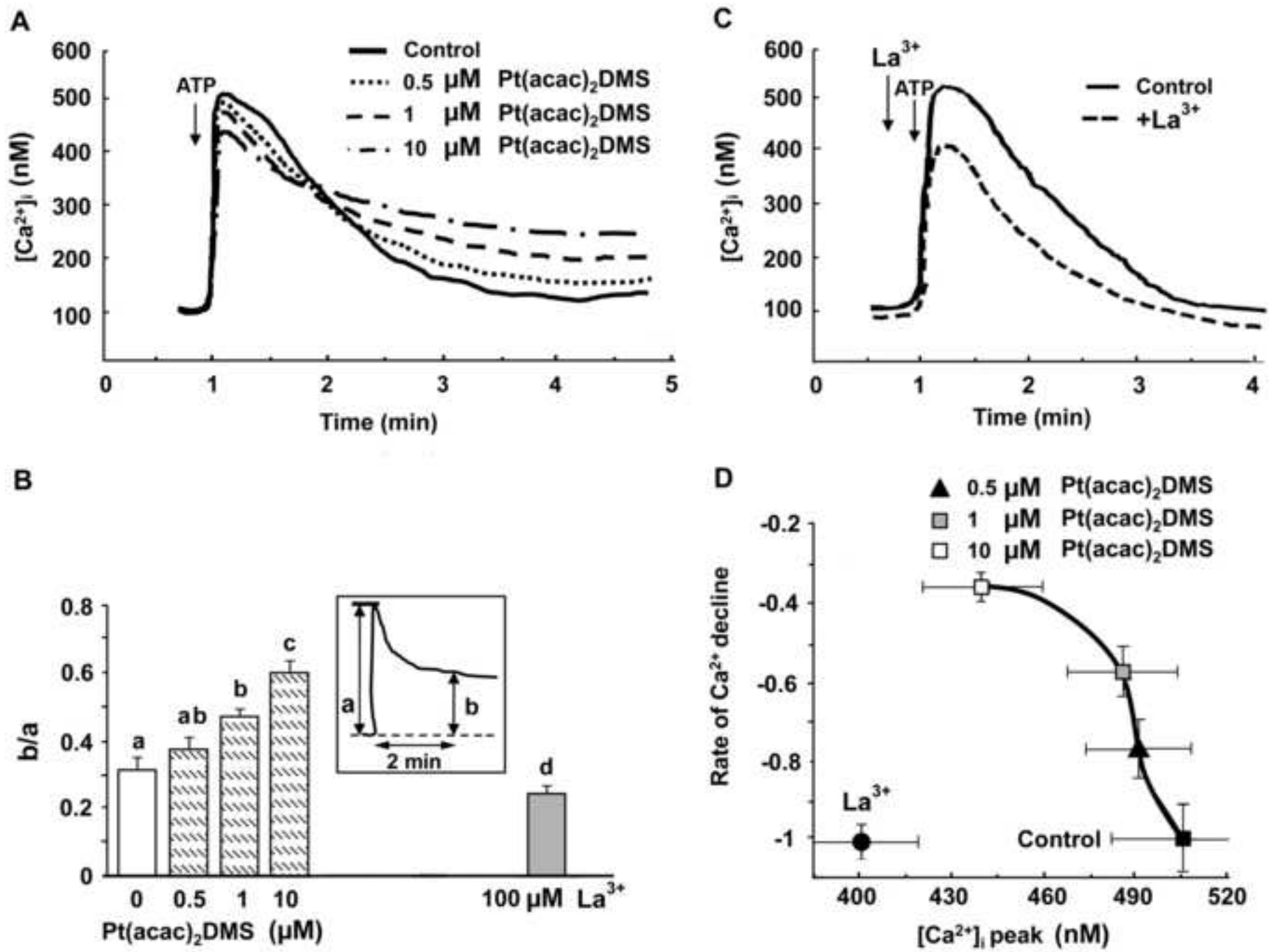


FIG. 4

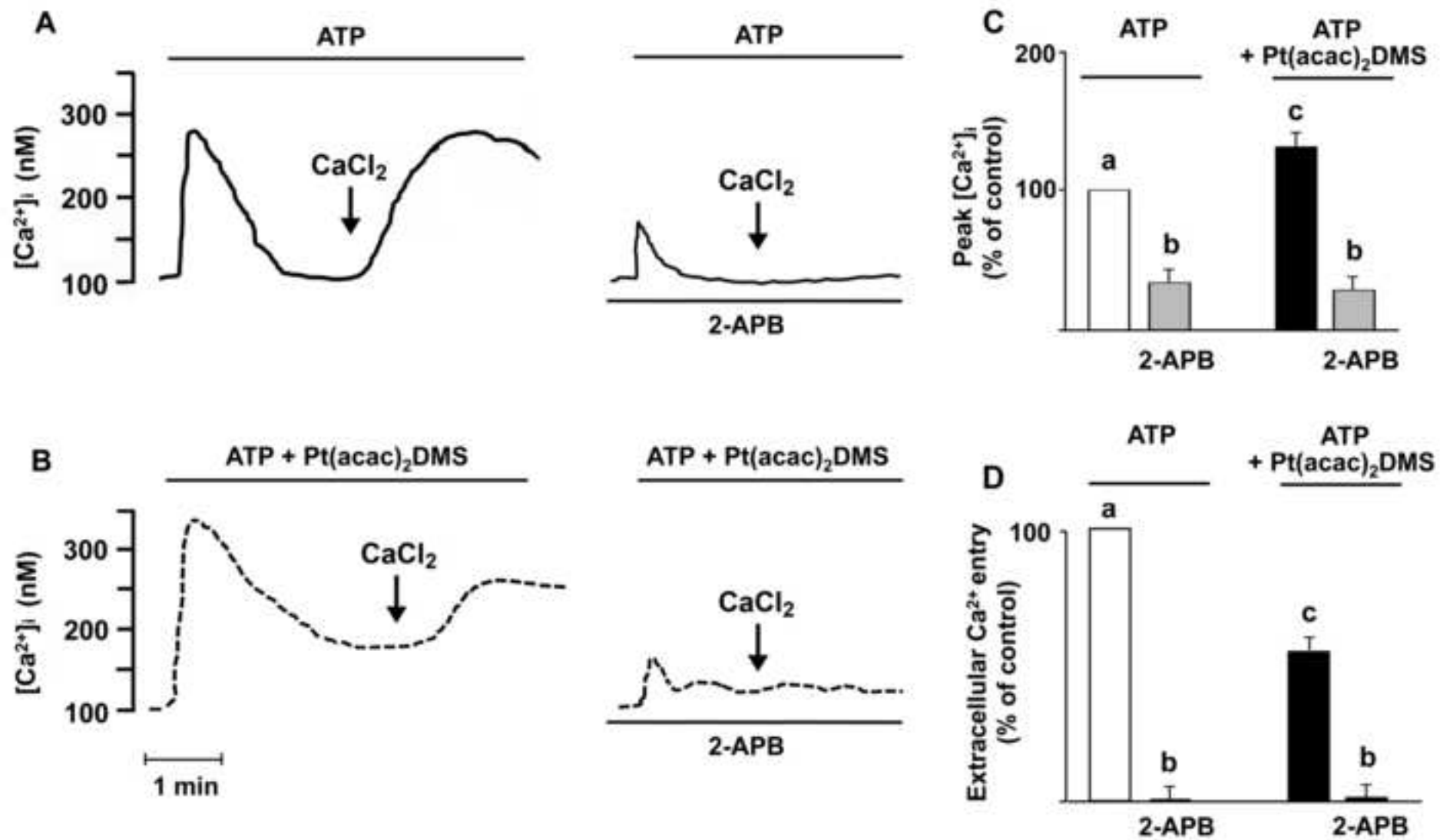


FIG. 5

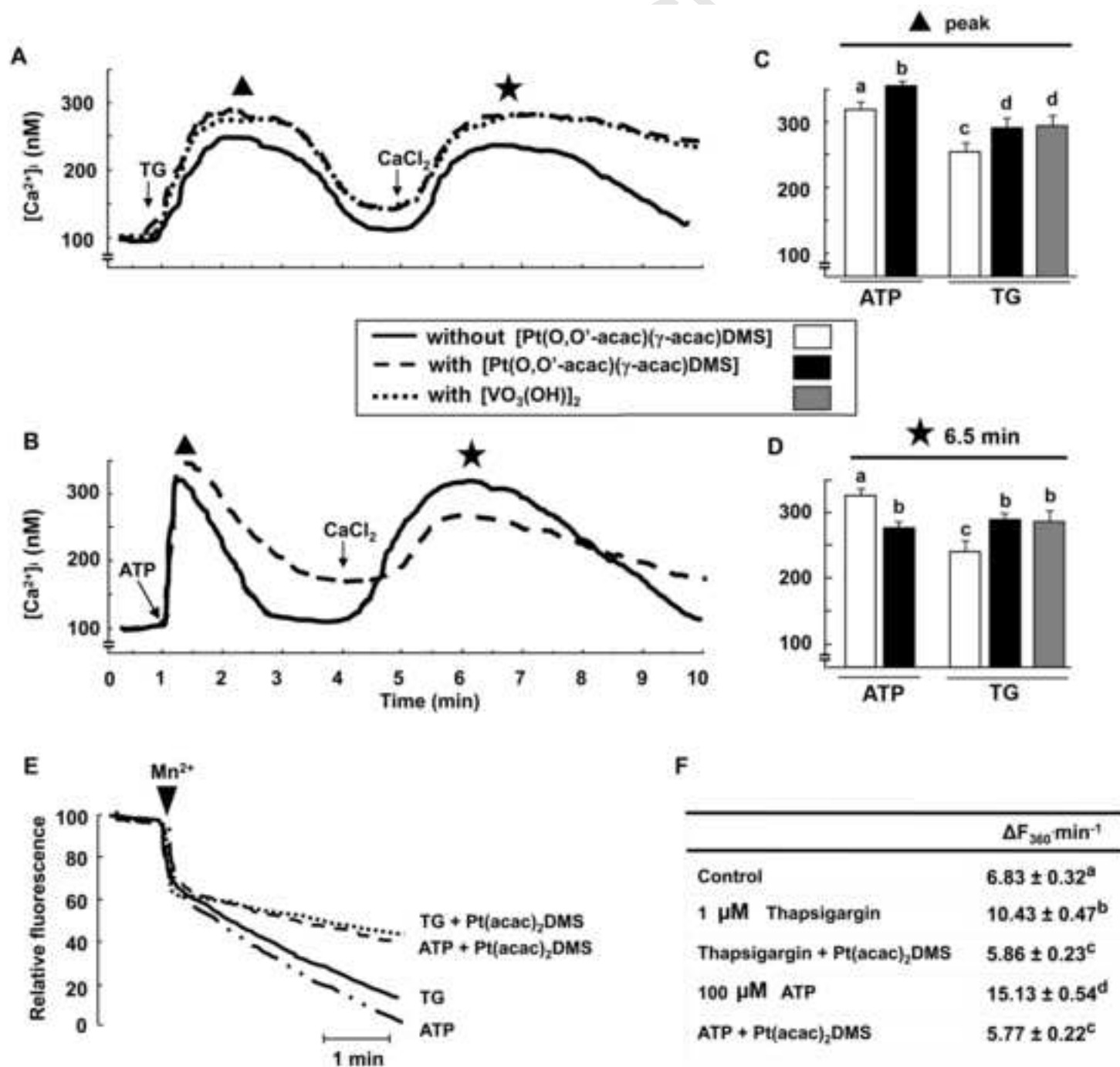


FIG. 6

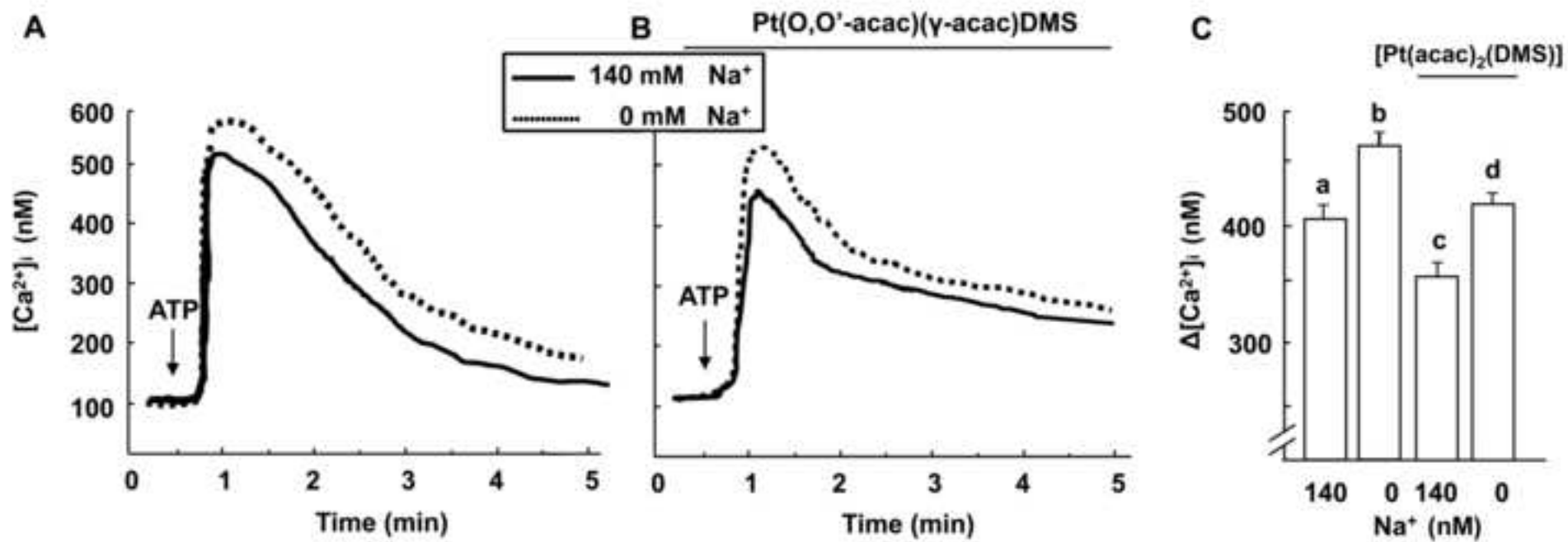


FIG. 7

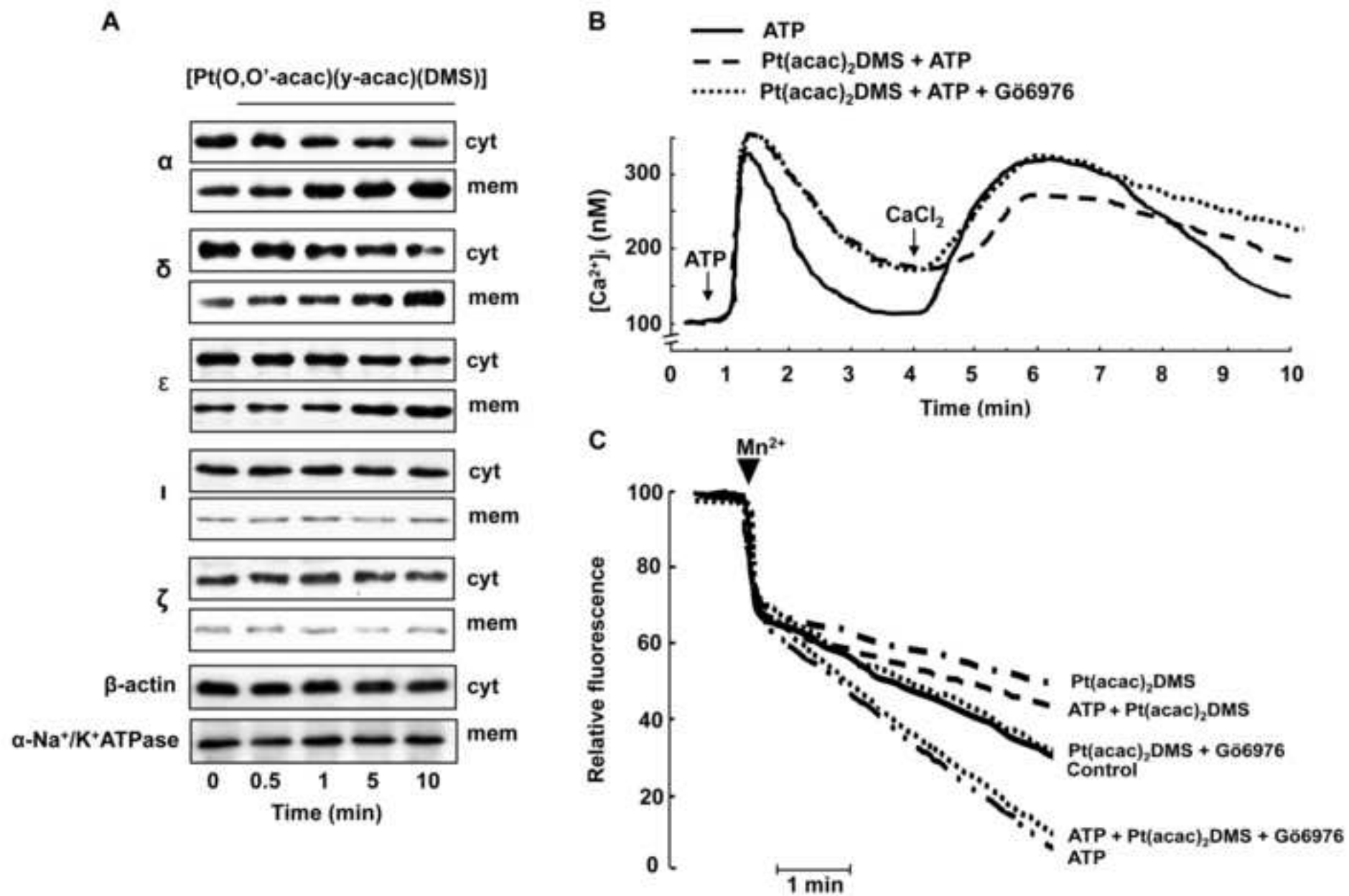


FIG. 8

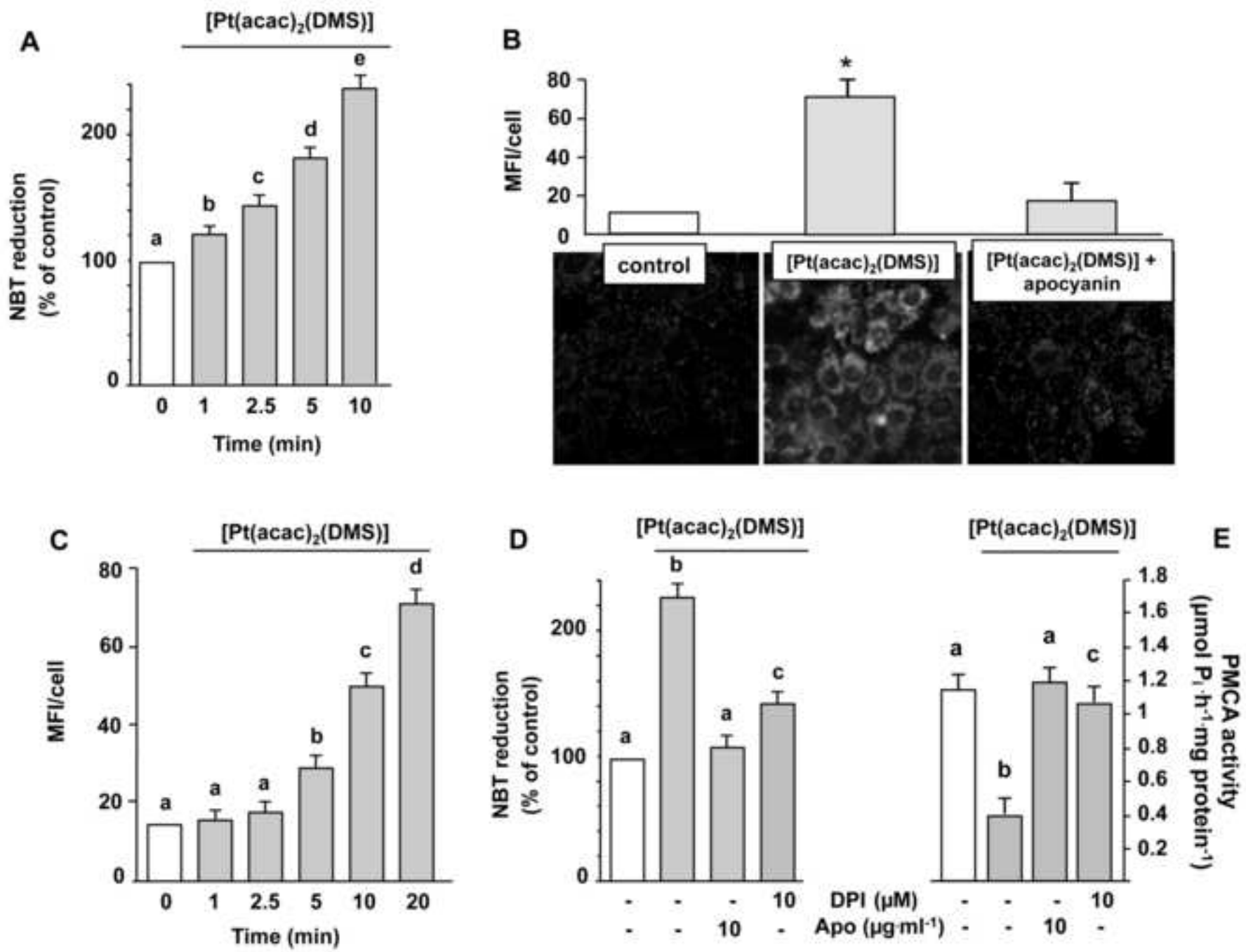


FIG. 9

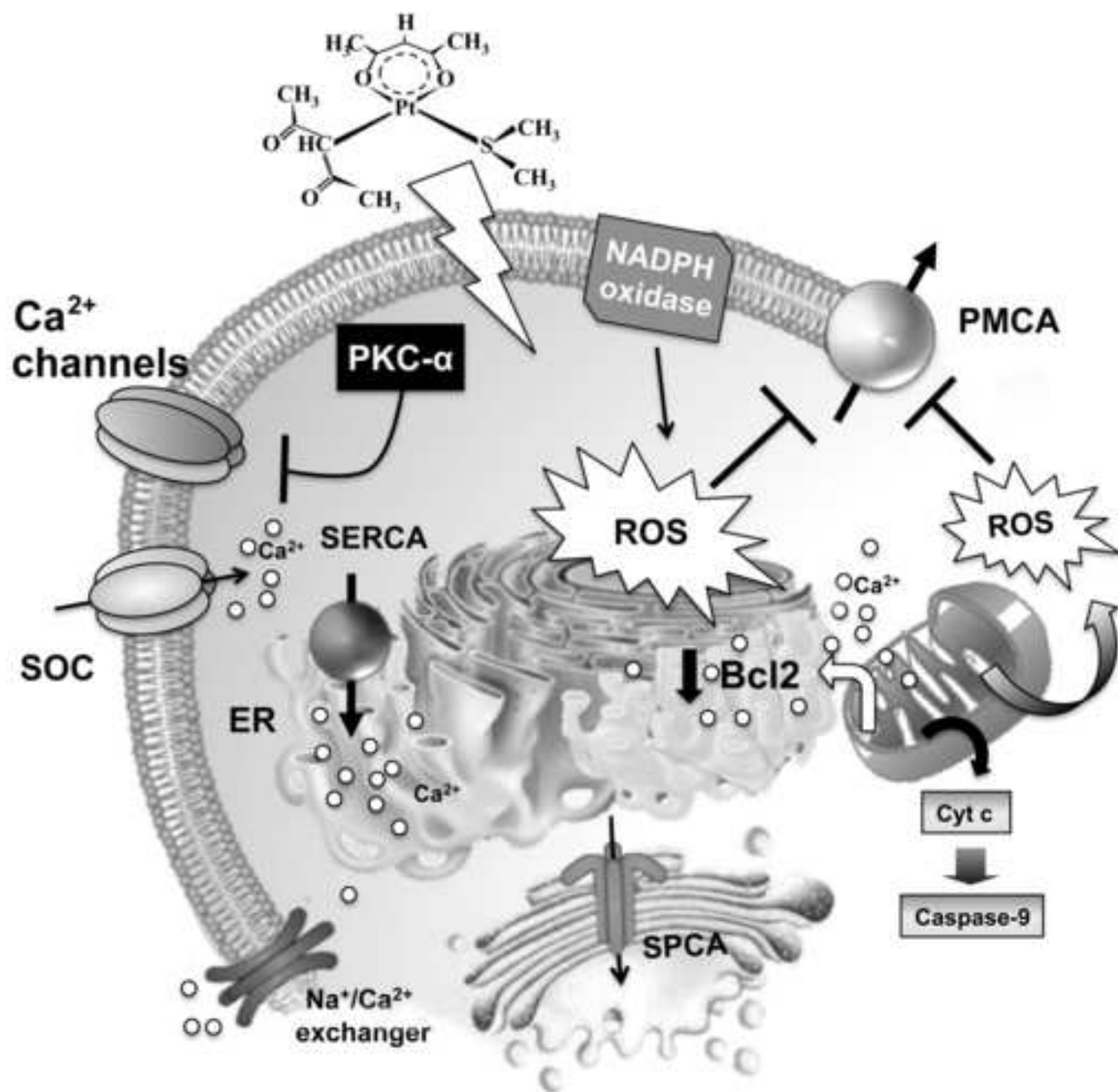


FIG.10

	MCF-7	SKBR-3	MDA- MB-231	MCF-10A
$\Delta[\text{Ca}^{2+}]_i$	151 ± 15^a	128 ± 13^a	132 ± 17^a	18 ± 4^b
$\Delta F_{360} \text{min}^{-1}$	-64 ± 9^a	-53 ± 7^a	-48 ± 7^a	-22 ± 3^b
$\Delta \text{PMCA activity}$	-75 ± 11^a	-62 ± 9^a	-66 ± 8^a	-28 ± 2^b
$\Delta \text{NBT reduction}$	140 ± 13^a	122 ± 11^a	113 ± 9^a	21 ± 5^b

TAB. I

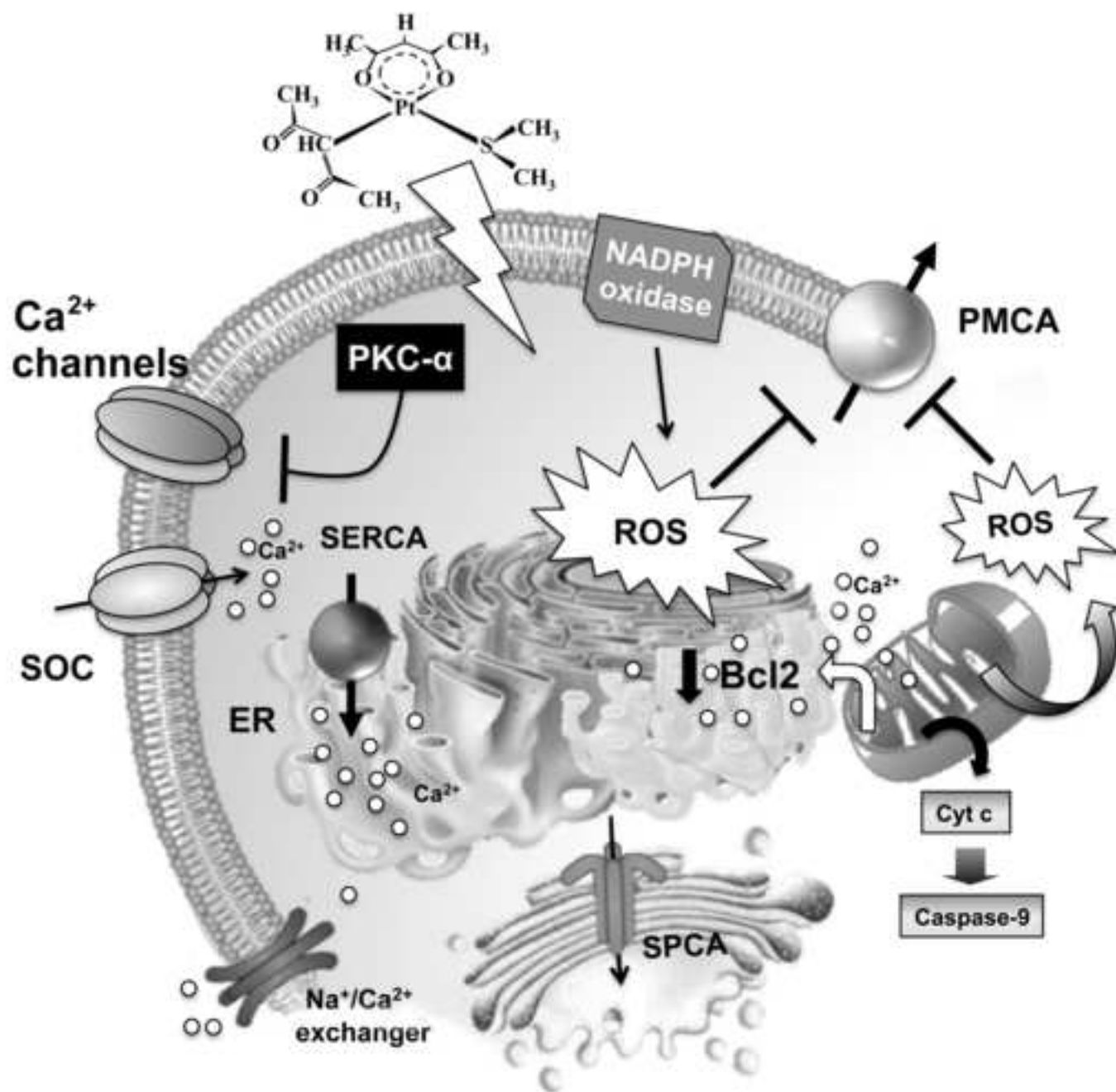


FIG.10